

PROJECT REPORT

On

**SYNTHESIS AND CHARACTERIZATION OF ZINC OXIDE-
GRAPHENE OXIDE COMPOSITE FOR ENHANCED
PHOTOCATALYTIC DEGRADATION AND ANTIBACTERIAL
ACTIVITY**

Submitted by

BINSHA PRINCE (AM22CHE003)

*In partial fulfillment for the award of the
Post graduate Degree in Chemistry*



**DEPARTMENT OF CHEMISTRY
AND
CENTRE FOR RESEARCH**

**ST. TERESA'S COLLEGE (AUTONOMOUS)
ERNAKULAM**

2023-2024

**DEPARTMENT OF CHEMISTRY
AND
CENTRE FOR RESEARCH
ST. TERESA'S COLLEGE (AUTONOMOUS)
ERNAKULAM**



M.Sc. CHEMISTRY PROJECT REPORT

Name : BINSHA PRINCE
Register Number : AM22CHE003
Year of Work : 2023-2024

This is to certify that the project “**SYNTHESIS AND CHARACTERIZATION OF ZINC OXIDE- GRAPHENE OXIDE COMPOSITE FOR ENHANCED PHOTOCATALYTIC DEGRADATION AND ANTIBACTERIAL ACTIVITY**” is the work done by **BINSHA PRINCE**.

Dr. Saritha Chandran A.
Head of the Department

Dr. Saritha Chandran A.
Staff-member in charge

Submitted to the Examination of Master's degree in Chemistry

Date:

Examiners:.....

:

**DEPARTMENT OF CHEMISTRY
AND
CENTRE FOR RESEARCH
ST. TERESA'S COLLEGE (AUTONOMOUS)
ERNAKULAM**



CERTIFICATE

This is to certify that the project work titled **“SYNTHESIS AND CHARACTERIZATION OF ZINC OXIDE- GRAPHENE OXIDE COMPOSITE FOR ENHANCED PHOTOCATALYTIC DEGRADATION AND ANTIBACTERIAL ACTIVITY”** is the work done by **BINSHA PRINCE** under the guidance of **Dr. SARITHA CHANDRAN A., HEAD OF THE DEPARTMENT**, Department of Chemistry and Centre for Research, St. Teresa's College, Ernakulam in partial fulfilment of the award of the Degree of Master of Science in Chemistry at St. Teresa's College, Ernakulam affiliated to Mahatma Gandhi University, Kottayam.

Dr. Saritha Chandran A.
Project Guide

Dr. Saritha Chandran A.
Head of the Department

**DEPARTMENT OF CHEMISTRY
AND
CENTRE FOR RESEARCH
ST. TERESA'S COLLEGE (AUTONOMOUS)
ERNAKULAM**



CERTIFICATE

This is to certify that the project work entitled **“SYNTHESIS AND CHARACTERIZATION OF ZINC OXIDE- GRAPHENE OXIDE COMPOSITE FOR ENHANCED PHOTOCATALYTIC DEGRADATION AND ANTIBACTERIAL ACTIVITY”** is the work done by **BINSHA PRINCE** under my guidance in the partial fulfilment of the award of the Degree of Master of Science in Chemistry at St. Teresa's College (Autonomous), Ernakulam affiliated to Mahatma Gandhi University, Kottayam.

Dr. SARITHA CHANDRAN A.
Project Guide

DECLARATION

I hereby declare that the project work entitled “**SYNTHESIS AND CHARACTERIZATION OF ZINC OXIDE- GRAPHENE OXIDE COMPOSITE FOR ENHANCED PHOTOCATALYTIC DEGRADATION AND ANTIBACTERIAL ACTIVITY**” submitted to Department of Chemistry and Centre for Research, St. Teresa’s College (Autonomous) affiliated to Mahatma Gandhi University, Kottayam, Kerala is a record of an original work done by me under the guidance of **Dr. SARITHA CHANDRAN A.,HEAD OF THE DEPARTMENT,** Department of Chemistry and Centre for Research, St. Teresa’s College (Autonomous), Ernakulam. This project work is submitted in the partial fulfillment of the requirements for the award of the Degree of Master of Science in Chemistry.

BINSHA PRINCE

Acknowledgements

The success and outcome of this project required a lot of guidance and assistance from many people, and I am extremely fortunate to have got this all throughout the period of my project work. I hereby take this opportunity to acknowledge all the people who kept forward in successfully completing this project.

First, I thank god almighty for the completion of work successfully, and his unlimited blessings throughout our life. Also I express my gratitude to my beloved Principal Dr. Alphonsa Vijaya Joseph and the Director, Rev (Sr) Dr. Vinitha CSST and the management for providing me the necessary facilities to successfully carry out our work.

I thank and express my sincere gratitude to Dr. Saritha Chandran A, Head of the department, Department of Chemistry and Centre for Research, St Teresa's College, Ernakulam for giving me all the support and guidance which made me complete the project duly.

I also express my heartfelt thanks to Mrs. Tiya K J in charge of Teresian Instrumentation and Consultancy Centre (TICC) for assisting me in different analysis.

Acknowledgements

I am thankful and fortunate enough to get constant encouragement, and remarkable suggestions throughout the project work from all the teaching staffs of my department.

Also I would like to extend my sincere esteems to all staffs in laboratory for their timely support and express my heartfelt thanks to my parents for their valuable support and prayers.

Finally, I would like to thank everybody who in their own way contributed in the successful realizations of the project.

BINSHA PRINCE

Acknowledgements

Contents

Chapter 1 Introduction	1
1.1 Nanotechnology	1
1.2 Graphene	3
1.2.1 Structure	3
1.2.2 Synthesis	4
1.2.3 Properties	5
1.2.4 Applications	6
1.3 Graphene Oxide	7
1.3.1 Structure	7
1.3.2 Preparation	7
1.3.3 Properties	10
1.3.4 Applications	11
1.4 Zinc Oxide	13
1.4.1 Properties	13
1.4.2 Structure	14
1.4.3 Applications	14
1.4.4 Preparations	17
1.5 ZnO-GO composites	19
1.5.1 Properties	19
1.5.2 Applications	22
1.5.3 Preparations	24
1.6 Applications	25
1.6.1 Photocatalytic activity of ZnO- GO composite	25
1.6.2 Antibacterial property of ZnO- GO composite	25

Chapter 2 Literature Review	27
------------------------------------	-----------

Chapter 3 Materials And Methods	31
3.1 Materials	31
3.3 Experimental methods	31
3.2.1 Green synthesis of Zinc Oxide nanoparticles	31
3.2.2 Synthesis of Graphene oxide nanoparticles	32
3.2.3 Synthesis of ZnO-GO nanoparticles	33
3.4 Characterization methods	34
3.4.1 Scanning Electron Microscopy (SEM)	34
3.4.2 X-RAY Diffraction (XRD)	35
3.4.3 Fourier Transform Infrared (FT-IR) Spectroscopy	36
3.4.4 Transmission Electron Microscopy (TEM)	37
3.4.5 UV- Visible Spectroscopy	38
3.5 Application	39
3.5.1 Photocatalytic degradation	39
3.5.2 Antibacterial activity	40

Chapter 4 Results and Discussion	43
4.1 Characterization of Zinc Oxide	43
4.1.1 XRD	43
4.1.2 FT-IR	48
4.1.3 HR- TEM	48
4.2 Characterization of Graphene oxide (GO)	49
4.2.1 XRD	49
4.2.2 FT-IR	52
4.2.3 HR- TEM	54
4.3 Characterization of ZnO- GO nanocomposite	54

4.3.1 XRD	54
4.3.2 FT-IR	59
4.3.3 HR- TEM	59
4.4 Photo degradation of Methylene blue	60
4.4.1 UV- Vis Spectroscopy	60
4.5 Antibacterial studies	62

Chapter 5 Conclusion	67
References	69

List of figures	
Fig 1.1 Graphene or single-layer graphite structure	4
Fig 3.1 ZnO nanoparticle	32
Fig 3.2 GO nanoparticle	33
Fig 3 ZnO- GO nanocomposite	34
Fig 4.1 XRD diagram of ZnO	43
Fig 4.2 FT-IR diagram of ZnO	48
Fig 4.3 TEM images of synthesized ZnO	49
Fig 4.4 XRD diagram of GO	49
Fig 4.5 FT- IR diagram of GO	52
Fig 4.6 FT-IR diagram of graphite	53
Fig 4.7 TEM images of synthesized GO	54
Fig 4.8 XRD diagram of ZnO-GO nanocomposite	54
Fig 4.9 FT-IR diagram of ZnO-GO nanocomposite	59
Fig 4.10 TEM images of ZnO- GO nanocomposite	60
Fig 4.11 UV-Visible absorption spectrum of Methylene blue	60
Fig 4.12 UV-Visible absorption spectrum of ZnO- GO composite	61

Fig 4.13 Antibacterial study done on <i>Salmonella Typhimurium</i>	62
Fig 4.14 Antibacterial study done on <i>Bacillus Cereus</i>	63
Fig 4.15 Antibacterial study done on <i>Clostridium Perfringens</i>	63
Fig 4.16 Antibacterial study done on <i>E. Coli</i>	63
Fig 4.17 Antibacterial study done on <i>S. Aureus</i>	63

List of tables	
4.1 Recorded values of 2θ , d values, FWHM, particle size of XRD diffractogram of ZnO	47
4.2 Recorded values of 2θ , d values, FWHM, particle size of XRD diffractogram of GO	51
4.3 Recorded values of 2θ , d values, FWHM, particle size of XRD diffractogram of ZnO-GO composite	56
4.4 Zone of inhibition of ZnO, GO and ZnO- GO composite	64

Abbreviations	
GO	Graphene oxide
ZnO	Zinc oxide
ZNP	Zinc nanoparticle
CNT	Carbon nanotube
LED	Light emitting diode
FWHM	Full width at half maximum
XRD	X-ray diffraction
SEM	Scanning electron microscopy
HR -TEM	High resolution transmission electron

Contents

	microscopy
FTIR	Fourier transform infrared microscopy
<i>S. Aureus</i>	<i>Staphylococcus Aureus</i>
<i>E. Coli</i>	<i>Escherichia Coli</i>
MB	Methylene blue

Contents

Chapter 1

Introduction

1.1 NANOTECHNOLOGY

The word nanotechnology is for the most part considered to be the understanding, control, and rebuilding of matter in nanometer scale (i.e., less than 100 nm) to make materials with properties and capacities. However, the word "nanotechnology" varies from field to field and country to country and is widely used as a "catch-all" description for anything very small [1]. Two basic approaches are included in the field of nanotechnology: (i) the "top-down" approach, which involves breaking down larger structures into smaller, composite parts or shrinking them to the nanoscale without atomic-level control; and (ii) the "bottom-up" approach, also known as "molecular nanotechnology" or "molecular manufacturing," which involves creating materials from atoms or molecular components through an assembly or self-assembly process. Molecular nanotechnology has significant promise for advancements in materials and manufacturing, electronics, energy, medicine and healthcare, biotechnology, information technology, and national security, even though most modern technologies rely on the "top-down" approach [2]. Nanoparticles can be divided into a large number of groups according to their size, shape, and makeup. Some classifications distinguish between inorganic

and organic nanoparticles; dendrimers, liposomes, and polymeric nanoparticles are classified as organic, whereas fullerenes, quantum dots, and gold nanoparticles are classified as the former. Based on their composition, different categories—such as carbon-based, ceramic, semiconducting, or polymeric—separate nanoparticles. Moreover, there are two types of nanoparticles: soft (liposomes, vesicles, and nanodroplets) and hard (fullerenes, titania [titanium dioxide], and silica [silica dioxide]).

Nanoparticles are typically categorized according to their intended function, such as fundamental research versus diagnosis or therapy, or according to the process by which they were created[3].

Numerous unique properties of nanoparticles are directly correlated with their size. Therefore, it makes sense that attempts have been made to include nanoparticles in composite materials to partially capture those qualities. The modern rubber tyre is an example of how the special qualities of nanoparticles have been applied to a nanocomposite material. Typically, rubber (an elastomer) is combined with an inorganic filler (a reinforcing particle), like silica or carbon black nanoparticles. The incorporation of nanoparticles is a complex procedure for the majority of nanocomposite materials. Agglomeration, the creation of huge clumps that are difficult to disperse, is a well-known tendency of nanoparticles. Furthermore, after being included in a composite material, nanoparticles may lose some of their distinctive size-related characteristics[4].

The use of nanoparticles increased significantly in the early 21st century, with nanocomposites seeing the fastest development despite manufacturing challenges. In the process of creating and designing novel materials,

nanocomposites were used as the building blocks for magnetic and dielectric (insulating) materials.

In addition to the benefits that nanotechnologies offer, there is a chance that they will have detrimental consequences on environmental security and human health. Although the whole impact of nano pollution on health is still unknown, harmful consequences on the pulmonary, reproductive, cardiac, digestive, cutaneous, and immunological systems have been identified. In addition, nanomaterials can pollute air, water, and—most importantly—soil. This type of pollution is persistent and difficult to detect, making nano pollution another unfavorable environmental outcome of man-made materials with unclear long-term effects. Before large-scale nanotechnology is fully established, larger, multicenter investigations are required to ascertain human reactions and the destiny of the nanoparticles in the environment.

1.2 GRAPHENE

1.2.1 STRUCTURE

A distinctive atomically thin 2D carbonaceous substance, graphene is thought to serve as the foundation for several carbonaceous materials, allotropes, including fullerenes, carbon nanotubes, graphene nanoplatelets, and graphite with varying dimensions. The 2D graphene hexagons in flat layers are represented by Fig valence band, which is attributed to the π -bonds and delocalized π -bonds that link each atom in a graphene sheet to its three nearest neighbours. The term "2D" refers to solids that possess strong in-plane chemical interactions but weak out-of- plane van der Waal's bonds. Graphene, a derivative of graphite, is a

derivative that finds extensive use in numerous cutting-edge fields of nanoscience and nanotechnology[5].

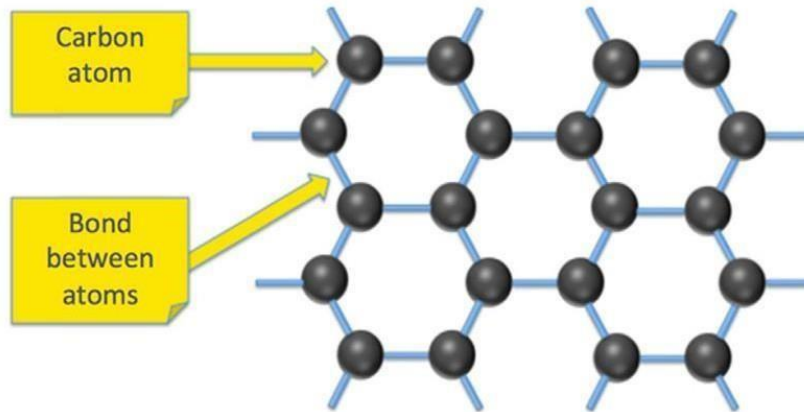


Fig. 1.1 Graphene or single-layer graphite structure

1.2.2 SYNTHESIS

Graphene can be synthesised in several ways. Most of them are top-down methods such as exfoliation and cleavage, thermal breakdown, chemical vapour deposition, chemically derived procedures, opening CNTs, thermal reduction, and oxidation-reduction, while bottom-up methods include molecular carbon precursor.

The graphene "gold rush" could begin with the growth of graphene crystals on top of substrates, their preparation in liquid suspension, or their acquisition as suspended membranes. Due to its versatility in functionalization and lack of metallic impurities, low-cost graphite precursors are now the primary source of cheap graphene produced in large quantities using oxidation, exfoliation, and reduction techniques [6].

1.2.3 PROPERTIES

The most remarkable of graphene's many characteristics are its high electrical and thermal conductivity, flexibility, toughness, lightweight, and resistance. These qualities constitute a true revolution and could be very helpful for innovation in many other fields. Here are a few instances:

- **High conductivity**

Batteries could have a ten-fold increase in usable life and faster charging times thanks to graphene, which would increase autonomy. Graphene will soon supplant a significant portion of the lithium batteries that are currently in use.

- **Lightness**

Drone batteries can also be made from graphene since they would be more durable and lighter. Reducing the weight of these energy-accumulating components might be a huge improvement since they are among the heaviest in the technology.

- **Transparency and flexibility**

At just 2%, graphene is a transparent material with extremely low light absorption. That, along with its flexibility, allowed flexible screens to be produced for a wide range of gadgets. Moreover, graphene is considerably less likely to break since it can be folded like cling film.

- High resistance

Significant advancements in the lighting industry are anticipated because graphene is a highly resistant substance in addition to being an excellent electric conductor. Graphene light bulbs, for instance, might extend the lifespan of each globe and use less energy than LED lights [7].

1.2.4 APPLICATIONS

- Graphene in building

The application of graphene in building materials has promise for enhancing building insulation. Furthermore, they might be stronger and more sustainable due to their increased resistance to fire, moisture, and corrosion. Construction materials would be refined, and environmentally friendly elements—like "green concrete," an eco-efficient substance that is more resilient and sustainable than the one utilised now—would be employed.

- Graphene in health

Fascinating uses of graphene exist in the fields of medicine and health. Stronger, more flexible, and lighter hearing aids could be created because of graphene's unique qualities. We might even be talking about creating new muscles and bones that would be added through surgery. Graphene oxide is still a work in progress, but it has the potential to be a useful tool for illness diagnosis and therapy. This element is produced when graphene undergoes oxidation, which transforms it into a substance with remarkable mechanical qualities.

- Graphene in electronics

The properties of graphene have the potential to revolutionise the electronics industry. By using this material, gadgets that are currently unattainable with today's components—smaller, lighter, harder, and more efficient—may be produced. Moreover, the use of graphene in electrical circuits would render the devices "immune" to moisture, which is a primary cause of deterioration. Its outstanding electrical and thermal conductivity is also a thousand times greater than copper's[8].

1.3 GRAPHENE OXIDE

1.3.1 STRUCTURE

Graphene oxide (GO) is derived from graphene, a two-dimensional form of carbon with a hexagonal lattice structure. While graphene possesses remarkable mechanical, electrical, and thermal properties, GO distinguishes itself by containing oxygen-functional groups like epoxides, hydroxyls, and carboxyls dispersed throughout its structure. These functional groups make GO hydrophilic and capable of dispersing in water-based solutions, expanding its potential applications in various fields such as electronics, energy storage, biomedicine, and environmental remediation [9].

1.3.2 PREPARATIONS

Various techniques have been developed to synthesize graphene oxide, each with its advantages and limitations:

1. Hummers Method:

Preparation of Oxidizing Mixture: In a round-bottom flask, potassium permanganate (KMnO_4) is added to concentrated sulfuric acid (H_2SO_4) while stirring in an ice bath. Sodium nitrate (NaNO_3) is gradually added to the mixture, maintaining the temperature below 10°C .

Addition of Graphite: Natural graphite flakes are slowly added to the oxidizing mixture under continuous stirring. The reaction proceeds at a low temperature ($\sim 0^\circ\text{C}$) to prevent excessive heat generation.

Oxidation: The mixture is stirred for several hours at a controlled temperature. The potassium permanganate and sulfuric acid react with graphite, leading to the insertion of oxygen-containing functional groups on the graphene sheets, forming graphite oxide.

Exfoliation: After oxidation, the mixture is poured into water and subjected to sonication or mechanical stirring to exfoliate the graphite oxide into individual graphene oxide sheets.

Washing and Purification: The resulting graphene oxide suspension is washed multiple times with water to remove excess reactants and acidic by-products. Purification may involve filtration and centrifugation to remove larger particles and impurities.

2. Brodie Method:

Preparation of Oxidizing Mixture: Fuming nitric acid (HNO_3) is placed in a round-bottom flask, and potassium chlorate (KClO_3) is slowly added while stirring. The reaction generates chloric acid, which is an oxidizing agent.

Addition of Graphite: Natural graphite flakes are added to the oxidizing mixture gradually, and the reaction is allowed to proceed at room temperature or slightly elevated temperatures.

Oxidation: The mixture is stirred for a specific duration, during which the graphite undergoes oxidation, leading to the formation of graphite oxide.

Exfoliation: Similar to the Hummers method, the resulting graphite oxide is exfoliated into graphene oxide sheets through sonication or mechanical stirring.

Washing and Purification: The exfoliated graphene oxide suspension is washed with water to remove excess reactants and acidic by-products, followed by purification steps to eliminate impurities.

3. Microwave-Assisted Oxidation:

Method: Creating the Graphite Oxide Precursor -A combination of acids, such as nitric acid (HNO_3) and sulfuric acid (H_2SO_4), is used to oxidise the graphite flakes.

Microwave Irradiation: The combination is exposed to microwave radiation for a predetermined amount of time and power. The solution is quickly heated by the microwave energy, which encourages graphite oxidation and the creation of I gave Grammarly the following AI prompts to help me with my writing:

Exfoliation and Purification: To exfoliate the graphite oxide into separate sheets, the suspension of graphene oxide is exposed to mechanical agitation or sonication following microwave treatment. The next steps involve washing and purification to get rid of extra reactants and contaminants[10].

4. Electrochemical Oxidation:

Procedure: Electrochemical cell preparation involves selecting an appropriate counter electrode and using graphite as the anode. A mixture of acids, such as phosphoric acid (H_3PO_4) and sulfuric acid (H_2SO_4), are commonly present in the electrolyte solution.

Electrochemical Oxidation: Graphite at the anode surface undergoes electrochemical oxidation when a voltage is placed between the electrodes. Graphene oxide is created when functional groups containing oxygen are added to graphene sheets.

Exfoliation and Purification: Using procedures like sonication and water washing that are detailed in previous methods, the resultant graphene oxide is exfoliated and purified[11].

1.3.3 PROPERTIES

Graphene oxide possesses unique properties that differentiate it from pristine graphene:

- **Mechanical Properties:** Although graphene boasts exceptional mechanical strength, GO experiences a decrease in mechanical properties due to the presence of defects and oxygen functional groups, which disrupt the carbon network. However, GO retains flexibility and can be easily functionalized to enhance specific mechanical properties.
- **Electrical Conductivity:** GO exhibits lower electrical conductivity compared to pristine graphene due to disruptions caused by oxygen-containing groups. However, conductivity can be partially restored through reduction processes, such as thermal, chemical, or

electrochemical reduction, which remove some oxygen functional groups.

- **Optical Properties:** Graphene oxide displays tunable optical properties based on the degree of oxidation and the density of functional groups present. These properties make GO suitable for applications in optoelectronics, photonics, and sensing.
- **Chemical Reactivity:** The presence of oxygen functional groups makes GO highly reactive, allowing for easy functionalization and integration of other molecules. This chemical versatility expands its potential applications in various fields, including biomedicine and environmental remediation[12].

1.3.4 APPLICATION

Graphene oxide finds diverse applications due to its unique properties:

- **Energy Storage:** Two examples of technologies that are being developed using materials based on graphene oxide and are the focus of extensive research are lithium-ion batteries and supercapacitors. GO's high electrical conductivity and vast surface area enable efficient charge storage and transmission.
- **Composite Materials:** GO is a good filler material in composite matrices due to its high aspect ratio, mechanical strength, and versatility when combined with other polymers and ceramics. These composites are used in the building, automotive, and aerospace industries because of their enhanced mechanical, thermal, and electrical properties.

- **Sensors:** Due to their great sensitivity and selectivity towards a variety of analytes, graphene oxide-based sensors have drawn a lot of interest. Utilising the special qualities of GO, gas sensors, biosensors, and environmental sensors have been created for a variety of uses, including environmental monitoring and medical diagnostics.
- **Biomedical Applications:** Graphene oxide has potential for use in bioimaging, tissue engineering, and drug delivery in the biomedical industry. It is a desirable option for next-generation therapies due to its biocompatibility, large surface area for drug loading, and capacity to functionalize with targeted ligands.
- **Environmental Remediation and Water Purification:** Materials based on graphene oxide have demonstrated remarkable efficacy in environmental remediation and water purification applications. Pollutants including organic dyes, heavy metals, and oil spills can be effectively absorbed by GO-based adsorbents, whereas GO membranes with precisely calibrated pore sizes are capable of filtering out large volumes of debris.
- **Optoelectronic Devices:** Graphene oxide is used in optoelectronic devices like solar cells, photodetectors, and light-emitting diodes (LEDs) because of its flexible substrate compatibility and tunable optical properties. It is useful for many different optoelectronic applications due to its broad spectral range of light absorption and emission capabilities[13].

1.4. ZINC OXIDE

Zinc oxide is an inanimate substance. It's a white, insoluble powder in water. Food supplements, cosmetics, rubber, plastic, ceramic, glass, cement, lubricants, paints, sunscreens, ointments, adhesives, sealants, pigments, batteries, ferrites, fire retardants, semiconductors, and first-aid tapes are just a few examples of the many materials and products that contain zinc oxide (ZnO). Although zinc oxide is found naturally as the mineral zincite, it is primarily manufactured.

1.4.1 PROPERTIES

Thermochromic change is the process by which crystalline zinc oxide goes yellow in the air and then back to white. Zinc oxide is an amphoteric oxide. Though most acids, including hydrochloric acid, may dissolve it, it is nearly insoluble in water. The right carboxylates, such as stearate or oleate, are formed when zinc oxide (ZnO) gradually reacts with the fatty acids in oils. Zinc hydroxy chlorides, or cement-like compounds, are the result of the reaction between ZnO and a strong aqueous solution of zinc chloride. This cement was used in dentistry. Zinc oxide has several beneficial properties, including strong room-temperature luminescence, a wide band gap, high electron mobility, and good transparency. Because of these characteristics, ZnO is useful for a wide range of novel applications, including transparent electrodes for liquid crystal displays, windows that save energy or block heat, and thin-film transistors and light-emitting diodes for electronics. At ambient temperature, ZnO has a comparatively broad direct band gap of ~3.3 eV. Higher breakdown voltages, the capacity to withstand strong electric fields, reduced electronic noise, and high-

temperature and high-power operation are benefits of having a wide band gap. ZnO's band gap can be adjusted further to $\sim 3\text{--}4$ eV by alloying it with cadmium oxide or magnesium oxide. Owing to this wide band gap, attempts have been made to use ZnO to produce solar cells that are observably transparent[14].

1.4.2. STRUCTURE

There are two primary forms of zinc oxide crystallization: cubic zincblende and hexagonal wurtzite. Due to its increased stability in ambient settings, the wurtzite structure is the most prevalent. ZnO can be grown on substrates with a cubic lattice structure to stabilize the zincblende form. The zinc and oxide centres in both instances have the most distinctive tetrahedral shape for zinc (II). At comparatively high pressures of approximately 10 GPa, ZnO transforms into the rock salt motif. Polymorphs of hexagonal and zinc blende lack inversion symmetry, meaning that a crystal does not become its reflection when it is reflected in a particular direction. The hexagonal and zinc blende ZnO exhibit piezoelectricity and pyroelectricity because of these and other lattice symmetry feature.

1.4.3. APPLICATION

- **The Rubber Industry**

In the rubber industry, ZnO is utilized to varying degrees. Sulphur is used to vulcanize rubber using stearic acid and zinc oxide. Rubber is protected against UV light and fungi by ZnO additives.

- Industry of Ceramics

In the ceramics industry, zinc oxide is widely utilized, particularly in glaze and frit compositions. ZnO's very low coefficient of expansion and its strong temperature stability, thermal conductivity, and comparatively high heat capacity make it a desirable material for ceramic production. Zinc oxide (ZnO) affects the optical properties and melting point of glazes, enamels, and ceramic compositions.

- Skin Care Regimen

Calamine lotion is made of zinc oxide mixed with approximately 0.5% iron (III) oxide (Fe_2O_3). Zincite and hemimorphite oxides have historically been combined to form the mineral calamine.

Many skin problems, such as atopic dermatitis, contact dermatitis, eczema-related irritation, diaper rash, and acne, are treated with zinc oxide. Products like calamine cream, anti-dandruff shampoos, baby powder, barrier creams for diaper rashes, and antibacterial ointments all include it. It is frequently mixed with castor oil to create an emollient and astringent lotion that is frequently applied to newborns.

- Antimicrobial

Zinc oxide is an antibacterial agent found in toothpastes and mouthwashes that is suggested to stop the formation of plaque and tartar and to reduce volatile sulfur compounds (VSC) and volatile gases in the mouth that cause bad breath. These products typically include zinc oxide or zinc salts and other active components such as essential oils, plant extracts, cetyl pyridinium chloride, xylitol,

hinokitiol, and Zinc oxide powder offers antimicrobial and deodorizing qualities. Cotton fabric, rubber, dental care items, and food packaging all contain ZnO. ZnO is not the only material where small particles exhibit enhanced antibacterial activity as compared to bulk material; silver and other materials also exhibit this property. The tiny particles' larger surface area gives rise to this characteristic.

- Sunscreen

Sunscreen contains zinc oxide, which absorbs UV radiation. The U.S. Food and Drug Administration (FDA) has approved it for use as a sunscreen and it is the broadest spectrum UVA and UVB absorber. It is also fully photostable. Zinc oxide prevents UVA (320–400 nm) and UVB (280–320 nm) rays of ultraviolet light when it is an ingredient in sunscreen. It is believed that zinc oxide and titanium dioxide, the two most popular physical sunscreens, are non-irritating, non-allergenic, and non-comedogenic. The skin does, however, absorb some zinc from zinc oxide. Because these tiny particles do not scatter light and appear white, zinc oxide and titanium dioxide nanoparticles are commonly found in sunscreens.

- Coatings

Metal surfaces have traditionally been shielded from corrosion by zinc oxide powder coatings. With galvanized iron, they perform very effectively. Iron interacts so rapidly with organic coatings that it becomes difficult to protect because it becomes brittle and loses its ability to adhere. Zinc oxide paints remain pliable and adhere for a long time on these kinds of surfaces. Zinc oxide doped with indium,

gallium, or aluminum at a high concentration (around 90% transparent, with a minimum resistivity of $\sim 10^{-4} \Omega \cdot \text{cm}$) is very conductive and transparent. ZnO: Al coatings are applied to windows to protect them from heat or to save energy. Depending on which side of the glass has the coating, it allows the visible portion of the spectrum to pass through while either reflecting infrared (IR) radiation return into the space (energy saving) or blocking it (heat protection) [15].

1.4.4 PREPARATION

- Sol-Gel method

Initially, a zinc acetate solution was made by mixing 20 gm $\text{Zn}(\text{CH}_3\text{COO})_2 \cdot 2\text{H}_2\text{O}$ with 150 ml distilled water and stirring for 20 minutes at 35 °C. Once more, to produce NaOH solution, 80 gm of powdered NaOH was weighed, combined with 80 ml of water, and agitated for around 20 minutes at 35 °C. Following the mixing of the two solutions, 100 ml of ethanol was added drop-wise while being vigorously stirred to carry out the titration process. The reaction was completed and a gel-like substance was obtained by continuing to agitate for around ninety minutes. Following an overnight drying at 80 °C, the gel was calcined for four hours at 250 °C in an oven. ZnO nanoparticles were then created.

- Chemical method

The zinc acetate precursor was refluxed for two and three hours in diethylene glycol (DEG) and tri-ethylene glycol (TEG), both with and without sodium acetate. The synthesized ZnO nanoparticles

were assessed using the following techniques: energy dispersive X-ray spectroscopy (EDX), field emission scanning electron microscopy (FESEM), transmission electron microscopy (TEM), thermogravimetric analysis (TGA), X-ray diffraction (XRD), UV visible spectroscopy, and Fourier transform infrared spectroscopy (FTIR)[14].

- Co-precipitation method

Zinc acetate [$\text{Zn}(\text{CH}_3\text{COO})_2 \cdot 2\text{H}_2\text{O}$] and sodium hydroxide [NaOH] are the raw ingredients needed to prepare ZnO. These two raw materials are dissolved in methanol in two different containers.

When synthesized, NaOH solution is added drop by drop while being sonicated in an ultrasonic bath to the translucent Zinc-Acetate solution. Throughout the reaction, the ultrasonic bath's temperature was kept at 30 °C. The reaction ends with the appearance of a white precipitate. Using a centrifuge, the final product was collected once the reaction had finished. To extract the precipitate from the unreacted raw materials has undergone multiple washings with ethanol and double-distilled water. In a box furnace, the ZnO NPs were finally placed in a crucible and annealed for three hours at 300 and 500 degrees Celsius. The sample numbers for these two samples are ZnO_S1 and ZnO_S2, respectively. Additionally, pure ZnO powders are annealed for three hours at 300 and 500 degrees Celsius [16].

1.5 ZnO -GO COMPOSITE

The exceptional characteristics of metal and metal oxide nanocomposites (MMO_x-NCs), namely their uniform size distributions, strong reactivity, and high surface area-to-volume ratios, have made them extremely attractive. Zinc oxide (ZnO) nanocrystals' superior optical performance and graphene oxide's (GO) absorption qualities allowed for the fabrication of ZnO and GO nanocomposites with synergistic photocatalytic effects using a precipitation process that uses GO as the catalyst carrier. X-ray diffraction, X-ray photoelectron spectroscopy, UV-vis spectroscopy, field emission scanning electron microscopy, transmission electron microscopy, and photocatalytic activity for the nanocomposites were used to characterize the produced composites. The findings demonstrate that ZnO is uniformly loaded onto GO's surface with the help of an efficient interface coupling. Electrons from the valence band of ZnO can move directly to the GO because of the interface interaction between ZnO. The composites have a 97.6% photodegradation efficiency, and the first-order reaction rate constant for photodegradation is 0.04401 min⁻¹. Next-generation graphene-based semiconductor composites can be constructed on a new platform thanks to the innovative ZnO-GO composites, which exhibit exceptional photocatalytic activity and show interesting future applications in the field of photocatalysis[17].

1.5.1. PROPERTIES

Zinc oxide-graphene oxide (ZnO-GO) composites have attracted a lot of interest lately because of the special qualities that result from the combination of graphene oxide and zinc oxide. When compared to their constituent parts, these composites have improved mechanical, electrical,

optical, and photocatalytic qualities. Comprehending these characteristics is essential for a multitude of uses, encompassing electronics and environmental restoration. We now examine the main characteristics of ZnO-GO composites:

- Electrical characteristics

Graphene oxide (GO) is a highly conductive substance, whereas zinc oxide (ZnO) is a semiconductor with a broad bandgap. as combined, the composite's electrical conductivity greatly increases as compared to pure ZnO, which makes it appropriate for use in energy storage, sensors, and photodetectors.

- Properties of Optics:

Because of its exceptional optical qualities, including its broad bandgap and great transparency, ZnO is a valuable material for optoelectronic applications. By increasing light absorption and lowering charge carrier recombination rates, GO integration in ZnO improves the composite's overall optical performance.

Applications in solar cells, light-emitting diodes (LEDs), and photovoltaic devices benefit from this feature.

- Mechanical Characteristics:

ZnO is mostly brittle, although graphene oxide has remarkable mechanical strength and flexibility. The mechanical characteristics of the composite are improved by incorporating GO into ZnO, leading to increased tensile strength and flexibility. Because of this, ZnO-GO composites can be used in wearable technology, flexible electronics, and structural materials that need to be both strong and flexible.

- **Properties of Photocatalysis:**
ZnO is a well-known photocatalyst that breaks down organic contaminants under UV light very well. ZnO's photocatalytic activity is increased when GO is added because it increases surface area and encourages charge separation. Environmental applications like air filtration, wastewater treatment, and self-cleaning surfaces take advantage of this characteristic.
- **Stability of Chemistry:**
ZnO nanoparticles are shielded from aggregation and chemical deterioration by graphene oxide, which also gives the composite chemical stability. This improves ZnO-GO composites' long-term stability and performance under varied environmental circumstances, making them appropriate for real-world uses demanding dependability and longevity.
- **Biocompatibility:**
Because ZnO-GO composites are so biocompatible, they can be used in biological applications like biosensing, tissue engineering, and drug delivery. The ability to bind biomolecules on the surface of GO facilitates tailored medicine delivery and high-sensitivity and specificity biological analyte sensing.
- **Modifiable attributes:**
ZnO-GO composites can have their qualities customized by varying their shape, content, and synthesis parameters. This tunability offers diversity and flexibility in design and optimization by enabling the material qualities to be adjusted to match particular application needs.

In conclusion, ZnO-GO composites have a special set of features that include chemical stability, biocompatibility, mechanical,

optical, and photocatalytic qualities. Their versatile characteristics render them auspicious contenders for an extensive array of uses, encompassing electronics, optoelectronics, environmental restoration, biomedicine, and additional fields. It is anticipated that future research and development in this area would broaden the possible uses and breadth of ZnO-GO composites[18].

1.5.2 APPLICATION

- **Photo catalysis**

The breakdown of organic pollutants in water and air is one of the photocatalytic applications for which ZnO-GO composites are utilized. The photocatalytic activity of ZnO is enhanced by the large surface area and high electron mobility of graphene oxide, which results in more effective destruction of contaminants under UV light.

- **Gas Sensors**

Because ZnO-GO composites have a high sensitivity and selectivity towards different gases, they have been used in gas sensors. With a wide surface area and improved electrical conductivity from graphene oxide and strong surface reactivity from ZnO, the combination is perfect for sensing gases like CO, NO₂, and NH₃.

- **Energy Storage**

These composites are used in energy storage devices like lithium-ion batteries and supercapacitors. Graphene oxide acts as a conductive network, facilitating fast electron transport, while ZnO

provides a high capacity for lithium storage or pseudo-capacitance for charge storage in supercapacitors.

- Photovoltaics

ZnO-GO composites are incorporated into solar cells to improve their efficiency. Graphene oxide acts as a charge transporter and enhances electron mobility, while ZnO serves as an electron acceptor. This synergistic effect enhances light absorption and charge separation efficiency, leading to higher power conversion efficiencies in photovoltaic devices.

- Antibacterial Applications

ZnO-GO composites have been explored for antibacterial coatings due to the antibacterial properties of both ZnO and GO. These composites can be used in medical devices, textiles, and packaging materials to inhibit the growth of bacteria and enhance hygiene.

- UV Shielding

ZnO-GO composites are used in sunscreen formulations and coatings for UV protection. Zinc oxide absorbs and scatters UV radiation, while graphene oxide provides mechanical strength and stability to the formulation. This combination offers effective protection against harmful UV rays.

- Water Purification

ZnO-GO composites are employed in water purification systems for removing heavy metals and organic contaminants. The high surface area and adsorption capacity of graphene oxide, combined with the photocatalytic activity of ZnO, enable efficient removal of pollutants from water.

Overall, the ZnO-GO composite material offers a wide range of applications across various fields, including environmental

remediation, energy storage, sensing, and biomedical applications, owing to its unique combination of properties derived from zinc oxide and graphene oxide[19].

1.5.3. PREPARATION

- Sol-gel hydrothermal method

After adding 50 ml of anhydrous ethanol to a beaker containing ZnO and sonicating for two hours, the ZnO dispersion was produced. After adding 50 ml of anhydrous ethanol to GO and sonicating it for two hours to produce an ethanol suspension, the graphene oxide ethanol suspension was added to the ZnO dispersion and agitated for twenty-four hours at a high temperature. Using anhydrous ethanol and centrifugation, the final product was cleaned. Next, 10 mL of anhydrous ethanol was used to redisperse the product once more. For a full day, ZnO-GO nanoparticles are obtained by vacuum drying [20].

- One-Pot hydrothermal method

The mass ratio used for the synthesis was GO:Zn(NO₃)₂. The one-pot hydrothermal method was used to create the three mass ratio changes, which were: 1:1 (0.2 g:0.2 g), 1:2 (0.2 g:0.4 g), and 1:8 (0.2 g:1.6 g). The process took two hours. We ultrasonicated the GO solid for one hour. After adding the Zn (NO₃)₂ in accordance with the ratio with 10 mL N₂H₄, the mixture was ultrasonicated for 30 minutes. After being moved to an autoclave, the solution was heated to 160 °C for two hours. Following a 15-minute

centrifugation at 4000 rpm, the GO/ZnO suspension was baked for three hours at 110 °C [21].

1.6 APPLICATIONS

1.6.1 PHOTOCATALYTIC ACTIVITY OF ZnO-GO COMPOSITE

Zinc oxide is an n-type semiconductor that serves as a photo catalyst due to its wide band gap, high electron excitation binding energy and high intrinsic electron mobility. Due to its ease of preparation, relatively low cost and high catalytic activity ZnO can be used as a substitute for TiO₂. Despite this the efficiency of ZnO is still low due to the factors such as its high resistivity, smooth recombination of photogenerated electron-hole pairs. In order to counter these effects and to enhance the photocatalytic activity in the UV region, the band gap needs to be narrowed. This can be made possible by making nano composites of ZnO with compounds such as GO. When combined with GO, the recombination of electron hole can be obstructed by acting as an electron acceptor. Moreover, due to the strong adsorption effect of GO, it can adsorb various organic dyes and thereby increase its photo degradation efficiency [22].

1.6.2 ANTIBACTERIAL PROPERTY OF ZNO-GO COMPOSITE

Antibacterial activity of the composite as well as the ZnO and GO was found out in gram-positive bacteria like *Staphylococcus Aureus*, *Bacillus Cereus*, and *Clostridium Perfringens* and gram-negative bacteria like *Escherichia Coli*, *Salmonella Typhimurium* by the well diffusion method. The antibacterial properties of zinc

oxide graphene oxide composite stem from their synergistic effects. Zinc oxide nanoparticles release zinc ions, known for their antibacterial action, disrupting bacterial cell membranes and inhibiting growth. Graphene oxide, with its high surface area and sharp edges, further enhances bacterial membrane disruption. The composite's unique structure and chemical properties create a hostile environment for bacterial survival, effectively reducing bacterial load. Studies have shown promising results in combating various bacterial strains, highlighting the potential of this composite in biomedical applications, such as wound dressings, medical implants, and water purification systems, offering a versatile and efficient solution to microbial control [23].

Chapter 2

Literature Survey

Nanobiotechnology is picking up huge impulse in this time owing to its capacity to tweak metals into their nano size, which productively changes their chemical, physical, and optical properties. **Jayanta Kumar Patra and Kwang-Hyun Baek** highlights different parameters influencing the union of nanoparticles by green nanobiotechnology and diverse methods utilized for characterizing the nanoparticles for their potential utilize in biomedical and natural applications [24].

Florence Sanchez and Konstantin Sobolev audits the current state of the field of nanotechnology in concrete and later key progresses. The potential of nanotechnology to make strides the execution of concrete and to lead to the advancement of novel, feasible, progressed cement-based composites with interesting mechanical, warm, and electrical properties is promising and numerous modern openings are anticipated to emerge within the coming a long time [25].

One of the many applications for inorganic nanoparticles is known: zinc oxide nanoparticles may be easily and sustainably generated. The biosynthesis of organisms that use metal nanoparticles has garnered increasing attention. Of these organisms, plants seem the most promising and are well-suited for the large-scale synthesis of nanoparticles. After synthesizing zinc oxide nanoparticles (ZnO-NPs) from hibiscus (*hibiscus rosa-sinensis*) leaves, **R. Sharma Devi and R. Gayathri** came to the

conclusion that the fast biological synthesis of zinc nanoparticles utilizing *Hibiscus rosa-sinensis* leaf extract is a simple, quick, and ecologically acceptable method for nanoparticle synthesis [26].

A popular technique for making graphene oxide (GO) is the Hummers' method, which uses potassium permanganate as the oxidant and concentrated sulfuric acid (H₂SO₄) as the intercalator. The findings of **Yonggang Hou, Shenghua Lv, Leipeng Liu and Xiang Liu** demonstrate that the types of oxygen-containing functional groups in the GO structure as well as the degree of oxidation of GO are directly influenced by the amounts of intercalator and oxidant [27].

The three methods used to create GO—Hummers', Intermediate, and Improved method—were combined, analyzed, and contrasted by **Nisha Yadav, Bimlesh Lochab**. In the former method, sulfuric acid and sodium nitrate are used, whereas in the latter, phosphoric acid and sodium nitrate are eliminated using non-oxidative Bronsted acids as an intercalant to exfoliate graphite and create a GIC intermediate that differs from Hummer's technique [28].

N.I. Zaaba, K.L. Foo, U. Hashim, S Tan, Wei-Wen Liu, C.H. Voon studied a modified Hummer's approach, which differs from the traditional Hummer's method, was used to extract graphite flakes and produce graphene oxide (GO). Using this approach, the experiment was conducted at ambient temperature without the need of an ice bath or sodium nitrate (NaNO₃) during synthesis [29].

Avinash R. Kachere, Prashant M. Kakade, Archana R. Kanwade, Priyanka Dani, Nandkumar T. Mandlik, Sachin R. Rondiya, Nelson Y. Dzade, Sandesh R. Jadkar, and Shivaji V. Bhosale, synthesized premium zinc oxide (ZnO) and graphene oxide (GO) nanocomposite (ZnO/GO nanocomposite) using a simple and efficient hydrothermal method. ZnO and GO were synthesized separately using the precipitation and modified Hummer's techniques, respectively. The effects of different GO concentrations on the optical and structural properties of ZnO nanoparticles were also investigated [30].

ZnO-GO nanocomposites were successfully created by precipitation using GO sheets as the catalytic carrier. The functional groups of GO serve as an anchor for the production of cross-linked ZnO nanoflakes on its surface. An extensive examination employing XRD, XPS, and SEM indicates that ZnO has been successfully decorated on the surface of GO. The photodegradation of MB dye from water was also studied using the generated nanocomposite. **Yi Lin, Ruoyu Hong, Huangiyin Chen, Di Zhang, and Jinjia Xu**, demonstrated that the annealed ZnO-GO nanocomposites' photocatalytic activity was superior to that of pure ZnO [31].

Hummer's method was successfully used to create the GO-ZnO nanocomposite. Using a range of methods, including FTIR, XRD analyses, and TGA, **H. Rehman, Z. Ali, T. G. Shahzady, A. Zahra, H. Hussain, A. Anwar, and M.S. Latif** examined the composite material's properties and verified its production. Using a synthetic material as a photocatalyst, the dyes RhB and MB were separated from their solutions. Using GO-ZnO as a photocatalyst, the removal efficiency of both dyes was evaluated by varying the dosage and duration [32].

Sangeetha Gunalan, Rajeshwari Sivaraj, and Venkatesh Rajendran demonstrate that, in comparison to chemical ZnO nanoparticles, green ZnO nanoparticles exhibit substantially enhanced biocidal activity against a variety of diseases. Additionally, if the particle dose, treatment duration, and production process are increased, so does the effectiveness of the nanoparticles. Based on the acquired results, it can be inferred that green ZnO nanoparticles have potential applications in agriculture and food safety as well as in future medicine [33].

Chapter 3

Materials and Methods

3.1 MATERIALS

The supplier of graphite powder and zinc nitrate hexahydrate was Nice Chemicals (P) Ltd, located in Kochi, Kerala. Hydrogen peroxide with an assay of 30% W/V was provided by Thermo Fisher Scientific India (P) Ltd, Mumbai. The assay of 98% W/V sulphuric acid, provided by Nice Chemicals (P) Ltd, Kochi, Kerala, was employed. Nice Chemicals (P) Ltd, Kochi, Kerala, provided Potassium permanganate. With a 99.9% W/V test, Changshu Hongheng Fine Chemicals Co. Ltd. produces ethanol in China, which was used in our experiments.

3.2 EXPERIMENTAL METHODS

3.2.1 Green synthesis of ZnO nanoparticles

Locally grown *Hibiscus rosa-sinensis* leaves were gathered. After being cleaned with water, the leaves were sun-dried. The leaves that had dried were ground into a fine powder. To create the leaf extract for the conversion of zinc ions to zinc oxide nanoparticles, 7.5g of finely powdered leaves and 150ml of distilled water were added to a 250ml glass beaker. After that, the mixture was heated to 70°C for an hour while being stirred magnetically, or until the solution turned pale yellow. After the extract had reached room temperature, it was filtered through a fresh cotton towel. A beaker containing 50ml of this extract was heated to a temperature between 60°C and 80°C with the use of a magnetic stirrer.

The solution was supplemented with 5g of zinc nitrate at reaching 60°C. After that, this mixture was reduced to a paste with a bright yellow colour by boiling it for 45 minutes. After that, this paste was gathered in a ceramic crucible and cooked for an hour at 400°C in a muffle furnace. Eventually, a white powder was produced, which was carefully gathered and packaged.



Fig. 3.1 ZnO nanoparticle

3.2.2 Synthesis of GO nanoparticle

GO was made using a modified Hummer's technique. One gram of graphite powder was added to 100ml of 98% H_2SO_4 in a beaker. At room temperature, it was stirred for twelve hours. After allowing the reaction mixture to cool to 10°C, 4g of KMnO_4 was gradually added. For 2.5 hours, the mixture was continuously agitated to keep the temperature below 10°C. After that, it was stirred for an hour and diluted with 50ml of distilled water. After that, 150ml of distilled water and 10 millilitres of 30% H_2O_2 were added to stop the process.

Once more, the reaction mixture was agitated at room temperature for five minutes. After cooling, the reaction mixture was transferred into a 1-litre beaker. This beaker was filled with enough distilled water to allow the

precipitate to settle properly. Following settling, the decantation procedure was carried out several times until the pH of the solution was neutral. After that, the precipitate was filtered and dried for six hours at 100°C in a muffle furnace. Therefore, GO nanoparticles were created.



Fig. 3.2 GO nanoparticle

3.3.3 Synthesis of ZnO-GO nanoparticle

The ZnO-GO nanocomposite was made via a hydrothermal process. The ZnO-GO nanocomposites were synthesized using ethanol and the previously obtained ZnO and GO nanoparticles as starting materials.

Initially, 200mg of ZnO and 10mg of the produced GO powder were divided among 10 and 20ml of ethanol, respectively. After that, these two solutions were thoroughly combined for an hour at room temperature (27°C) using an ultrasonic bath. After that, the mixture was placed in a 100ml autoclave lined with Teflon and heated to 180°C for 24 hours. To create ZnO-GO nanocomposites, the final products were centrifuged, cleaned in ethanol and distilled water, and then dried for 12 hours at 60°C in a hot air oven [34].



Fig. 3.3 ZnO-GO nanocomposite

3.4 CHARACTERIZATION METHODS

3.4.1 SCANNING ELECTRON MICROSCOPE (SEM)

By scanning an object's surface to create a high-resolution image, scanning electron microscopy, or SEM, creates detailed, magnified images of that thing. SEM does this by using a focused electron beam. The created images offer information about the object's composition and physical attributes. The instrument utilised to obtain this composition and topography data is a scanning electron microscope. SEM is a useful and practical technique with many uses across many sectors and businesses. Both artificial and naturally existing materials can be analysed using it. The 6390LV device that was fitted has an accelerating voltage range of 0.5 KV to 30 KV and a resolution of 4nm (30 KV). a 3,00,000 Eda magnification is added. The core components of the SEM are the specimen stage, secondary electron detector, electron gun, condenser and objective lens, image display, recording, and vacuum system.

3.4.2 X-RAY DIFFRACTION (XRD)

A technique for examining a material's crystal structure is X-ray diffraction (XRD). It offers helpful details about the average particle size, lattice constant, and crystal phase of nanoparticles. The foundation of X-ray diffraction is the constructive interference of monochromatic X-rays with a crystalline material, such as a single crystal or powder. A cathode beam tube produces the monochromatic X-rays, which are at that point sifted to make monochromatic radiation, collimated to concentrate, and coordinated towards the test. The atomic electrons in a crystal are accelerated and sent into vibration when a monochromatic X-ray strikes it.

These electrons accelerate and then discharge radiation at a frequency equal to the incident X-rays in all directions. The X-rays that are produced are in phase with each other if the incident radiation's wavelength is greater than the crystal's dimensions.

Nevertheless, the radiation that the electrons generate is out of phase with one another since the dimensions of an atom are almost the same as the wavelength of an X-ray. These radiations have the potential to interfere either constructively or destructively, creating peaks and minima in a diffraction pattern in particular directions.

The Bragg's equation can be used to analyze the phenomenon.

$$2d_{hkl} \sin \theta = n\lambda$$

where n is diffraction order (1, 2, 3, and so on), d is the distance between lattice planes of atoms in the crystal, θ is the diffraction angle, and λ is the wavelength of the X-rays used.

The outcome is a row of diffraction peaks responding with relative intensities that fluctuate together with a certain value of 2θ , which is the diffractogram pattern. The relative strength of the peak series is determined by the quantity and distribution of atoms or ions within the unit cell of the material. The crystalline material under study can be recognized by the diffraction pattern that was acquired. As a result, the approach offers great information about the dimensions of the unitcell and the type of lattice under investigation.

3.4.3 FOURIER TRANSFORM INFRARED (FTIR) SPECTROSCOPY

Fourier-transform infrared spectroscopy (FTIR) can provide crucial information on the surface functional groups and chemical composition of nanoparticles during their characterization. What to expect from a nanoparticle FTIR analysis is:

Functional Group Identification: Using Fourier Transform Infrared Spectroscopy (FTIR), certain functional groups on the surface of nanoparticles, such as hydroxyl, carboxyl, or amine groups, can be identified. Chemical composition: It helps determine the chemical composition of the nanoparticle and confirms the presence of specific compounds or coatings. Surface Modifications: By identifying any changes in the nanoparticle surface caused by coatings or modifications, FTIR can be used to assess the success of functionalization. Interactions: It clarifies the nature of the interactions between stabilisers, surfactants, and other substances withnanoparticles. Purity: FTIR can also be used to assess the purity of

generated nanoparticles by identifying any unwanted or impurity-containing compounds.

All things considered, FTIR analysis helps to optimize synthesis processes and applications by offering a comprehensive understanding of surface chemistry, functionalization, and interactions in nanoparticle characterization.

Fourier-transform infrared spectroscopy (FTIR), a powerful analytical technique, can be used to determine the chemical bonds in a sample by measuring the absorption of infrared radiation. In FTIR spectroscopy, a sample is exposed to an infrared light beam, and the amount of light absorbed at each wavelength is recorded. The sample's molecular composition enables it to absorb specific infrared wavelengths, resulting in a unique spectrum that serves as a material fingerprint. By comparing this spectrum with reference spectra, researchers can determine the presence of functional groups in the material and identify new compounds. The study of molecular vibrations and interactions as well as qualitative and quantitative analysis are common uses of FTIR in a number of fields, including chemistry, pharmacology, forensic science, and materials research[35].

3.4.4 TRANSMISSION ELECTRON MICROSCOPY (TEM)

The transmission electron microscope finds application in the study of semi-conductors, nanoparticles, nanotubes, virology, material science, cancer, and pollution control. This type of microscopy produces a picture by passing an electron beam through a material. The specimen is typically an ultrathin slice, less than 100 nm thick,

or a suspension on a grid. A picture is produced when the electrons in the sample interact with the beam as it travels through it.

The picture is at that point amplified and focussed onto an imaging gadget, which may be a fluorescent screen, a layer of photographic film, a coordinate electron finder, or a scintillator coupled to a charge-coupled gadget. The installed model, JEM -2100, employs a LaB6 electron cannon and has an acceleration voltage of 200 kV and a resolution of 0.24 nm. In addition to producing 2D images that are simpler to understand than 3D SEM images, TEMs also provide higher-resolution images and offer atomic and crystallographic data. Furthermore, they enable users to investigate extra features of a particular sample.

3.4.5 UV-VISIBLE SPECTROSCOPY

The ultraviolet/visible region (UV-Vis) can be measured at wavelengths between 200 and 800 nm. A molecule experiences changes in its electrical energy levels as it absorbs ultraviolet or visible light. It is possible to characterize the optical and electrical characteristics of a broad variety of materials, such as films, powders, liquids, and monolithic solids.

UV-vis spectroscopy is an analytical method that may be applied to a range of organic molecules and certain inorganic species. It is inexpensive, straightforward, adaptable, and non-destructive. UV-vis spectrophotometers compute the absorption or transmission of light through a material based on its wavelength. UV-vis finders are utilized to measure and classify the concentration of compounds in fluid streams in high-performance liquid chromatography and ultra-high-performance liquid chromatography. It makes it possible to

identify any animal by combining these techniques with mass spectrometry. Typical hot solids emit radiation with a variety of wavelengths, which is mostly influenced by the solid's temperature. The concept of chance allows for the prediction of the energy released at each wavelength.

When incident radiation interacts with the electron cloud in a chromophore, it can promote one or more outer shell electrons or bond electrons from a ground state into a higher energy state, resulting in an electronic transition that produces UV-visible (UV-Vis) spectra. Large visible and UV spectral bands are typical of substances, and they may not show excellent compound recognition accuracy. Nonetheless, they are suitable for quantitative experiments and provide a helpful fallback approach for drug detection.

3.5 APPLICATION

3.5.1 PHOTODEGRADATION OF METHYLENE BLUE

For the study of photodegradation, a methylene blue solution was prepared by adding 10 mg of dye to 1 litre of distilled water. 200 ml of this solution was transferred equally into two clean 250 ml beakers. About 20 mg of the synthesized ZnO-GO composite was added to one of the beakers and stirred well. The other one was kept blank to study the degradation of MB alone. These dispersions were kept under the exposure of sunlight. At regular intervals, the absorbance of solutions was measured using UV-Vis spectrophotometer.

3.5.2 ANTIBACTERIAL ACTIVITY OF ZINC OXIDE GRAPHENE OXIDE COMPOSITE

- Preparation of nutritional media

One hundred milliliters of distilled water were used to dissolve 1.3 grammes of nutritional broth to create the soup. Five milliliters of nutritional broth were placed within test tubes, which were then autoclave-sterilized. In 100 milliliters of distilled water, 1.3 grams of nutrient broth and 2 grams of agar-agar were combined to create nutrient agar media. After the media had been autoclaved, sterile petriplates were filled with 20 ml of each medium under aseptic circumstances.

- Preparation of microbiological cultures

The test organisms, which included *Salmonella Typhimurium*, *E. Coli*, *S.Aureus*, *Bacillus Cereus*, and *Clostridium Perfringens*, were inoculated into five milliliters of nutritional broth that had been sterilised. The incubation period was one night at 37°C.

Saturated solution of ZnO, GO and composite was prepared by dissolving 0.1g in 5ml water. These solutions were then kept in the ultrasonicator for 30 minutes. Then the antibacterial studies of this were studied using gram-positive bacteria like *S. Aureus*, *Bacillus cereus*, and *Clostridium Perfringens* and gram-negative bacteria like

E. Coli, *Salmonella Typhimurium* by the well diffusion method.

- Well diffusion method

Cotton swabs that had been sterilised were used to create a grass culture of every bacteria. After being dipped into the bacterial suspension and wiped from top to bottom, a sterile swab was used to ensure that no area remained uncontaminated. To cover the entire plate with germs, the plate was rotated 90 degrees and the same process was carried out again. After the grass was ready, sterile well cutters were used to cut 6 mm diameter wells into agar plates.

Following the labelling of the wells, 20µL of the sample (ZnO, GO, and ZnO-GO composites) were added to the appropriate wells. The antibacterial efficacy of the ZnO, GO, and ZnO-GO composite samples was evaluated in comparison to the commonly used antibiotics. For 24 hours, this plate was incubated at 37°C. A standard ruler was used to measure each zone's radius in cm. No colonies will form if the substance is efficient against bacteria at a particular concentration. This zone of inhibition serves as a gauge for the compound's potency; there is more clear space surrounding the well, the more potent the molecule is.

- Killing and disposing

Following the experiment, the plates are autoclaved for 20 minutes to kill the bacteria. To eliminate any potential microorganisms, every piece of glassware utilized in the experiment underwent autoclaving[36].

Chapter 4

Results and discussion

4.1 CHARACTERIZATION OF ZINC OXIDE

4.1.1 XRD

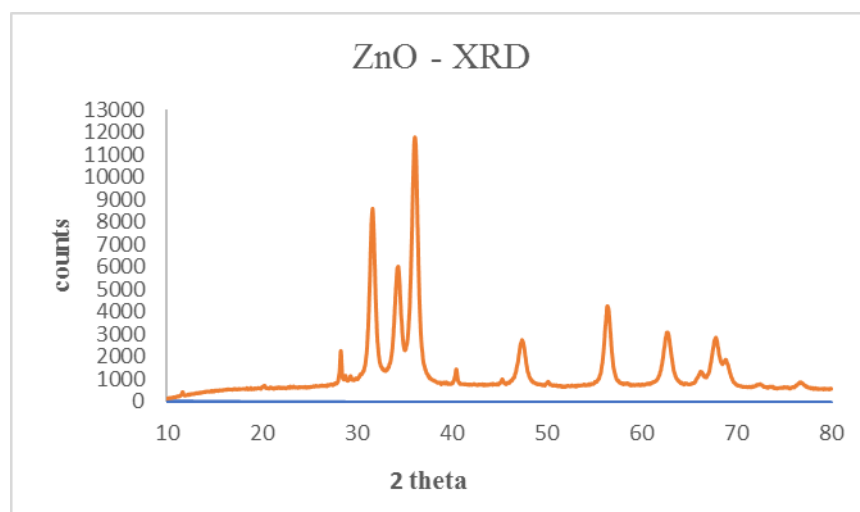


Fig 4.1 XRD diagram of ZnO

The XRD of the synthesized ZNPs is given in figure 4.1. The design clearly shows the crystalline structure of the synthesized nanoparticles. The sharp diffraction crests were watched at 2θ values 31.689, 34.360, 36.169, 47.465, 56.500, 62.789 & 67.842 degrees. These crests are ordered as (100), (002), (101), (102), (110), (103) & (112) diffraction grid planes separately which affirm the hexagonal wurtzite structure for the synthesized nanoparticles. This design is in understanding with the standard crests shown by the Universal Middle for Diffraction

Information. The normal estimate of ZNPs was calculated from the most elevated strongly top (101) utilizing the Debye–Scherrer condition, where λ is the X-ray wavelength coming from Cu-K α (1.54060 Å), β is the complete width at half maxima of the diffraction top in radians, θ is the Bragg's point in degrees, and K is the shape calculate and its esteem is rise to 0.9.

$$D = \frac{K \times \lambda}{\beta \cos \theta}$$

Peak 1

$$2\theta = 31.689^\circ$$

$$\theta = 15.8445 = 0.2765 \text{ radian}$$

$$\cos \theta = 0.9999$$

$$\beta = 0.547 = 0.0095 \text{ radian}$$

$$\lambda = 1.5406 \times 10^{-10} \text{ m}$$

From Debye Scherrer Equation,

$$D_1 = \frac{0.9 \times 1.5406 \times 10^{-10} \text{ m}}{0.0095 \times 0.9999} \\ = \underline{\underline{14.5966 \text{ nm}}}$$

Peak 2

$$2\theta = 34.360^\circ$$

$$\theta = 17.18 = 0.2998 \text{ radian}$$

$$\cos \theta = 0.9999$$

$$\beta = 0.648 = 0.0113 \text{ radian}$$

$$\lambda = 1.5406 \times 10^{-10} \text{ m}$$

From Debye Scherrer Equation,

$$D_2 = \frac{0.9 \times 1.5406 \times 10^{-10} \text{ m}}{0.0113 \times 0.9999} \\ = \underline{\underline{12.2715 \text{ nm}}}$$

Peak 3

$$2\theta = 36.169^\circ$$

$$\theta = 18.0845 = 0.1356 \text{ radian}$$

$$\cos \theta = 0.9999$$

$$\beta = 0.683 = 0.0119 \text{ radian}$$

$$\lambda = 1.5406 \times 10^{-10} \text{ m}$$

From Debye Scherrer Equation,

$$D_3 = \frac{0.9 \times 1.5406 \times 10^{-10} \text{ m}}{0.0119 \times 0.9999}$$
$$= \underline{\underline{11.6528 \text{ nm}}}$$

Peak 4

$$2\theta = 47.465^\circ$$

$$\theta = 23.7325 = 0.4142 \text{ radian}$$

$$\cos \theta = 0.9999$$

$$\beta = 0.831 = 0.0145 \text{ radian}$$

$$\lambda = 1.5406 \times 10^{-10} \text{ m}$$

From Debye Scherrer Equation,

$$D_4 = \frac{0.9 \times 1.5406 \times 10^{-10} \text{ m}}{0.0145 \times 0.9999}$$
$$= \underline{\underline{9.5633 \text{ nm}}}$$

Peak 5

$$2\theta = 56.500^\circ$$

$$\theta = 28.25 = 0.4931 \text{ radian}$$

$$\cos \theta = 0.9999$$

$$\beta = 0.747 = 0.0130 \text{ radian}$$

$$\lambda = 1.5406 \times 10^{-10} \text{ m}$$

From Debye Scherrer Equation,

$$D_5 = \frac{0.9 \times 1.5406 \times 10^{-10} \text{ m}}{0.0130 \times 0.9999}$$

$$= \underline{\underline{10.6668 \text{ nm}}}$$

Peak 6

$$2\theta = 62.789^\circ$$

$$\theta = 31.3945 = 0.5479 \text{ radian}$$

$$\cos \theta = 0.9999$$

$$\beta = 0.89 = 0.0155 \text{ radian}$$

$$\lambda = 1.5406 \times 10^{-10} \text{ m}$$

From Debye Scherrer Equation,

$$D_6 = \frac{0.9 \times 1.5406 \times 10^{-10} \text{ m}}{0.0155 \times 0.9999}$$

$$= \underline{\underline{8.9463 \text{ nm}}}$$

Peak 7

$$2\theta = 67.842^\circ$$

$$\theta = 33.921 = 0.5920 \text{ radian}$$

$$\cos \theta = 0.9999$$

$$\beta = 0.747 = 0.0130 \text{ radian}$$

$$\lambda = 1.5406 \times 10^{-10} \text{ m}$$

From Debye Scherrer Equation,

$$D_7 = \frac{0.9 \times 1.5406 \times 10^{-10} \text{ m}}{0.0130 \times 0.9999}$$

$$= \underline{\underline{10.6668 \text{ nm}}}$$

$$\text{Average Size} = \frac{14.5966 + 12.2715 + 11.6528 + 9.5633 + 10.6668 + 8.9463 + 10.6668}{7}$$

$$= \underline{\underline{11.1949 \text{ nm}}}$$

Table 4.1 Recorded values of 2θ, d value, FWHM, particle size of XRD diffractogram

Peaks (2θ) (Degree)	d values	FWHM (β)	Particle Size D (nm)	Average Particle Size (nm)
31.689	2.8213	0.547	14.5966	11.195
34.360	2.6079	0.648	12.2715	
36.169	2.4815	0.683	11.6528	
47.465	1.9140	0.831	9.5633	
56.500	1.6274	0.747	10.6668	
62.789	1.4787	0.890	8.9463	
67.842	1.3803	0.747	10.6668	

XRD analyses revealed the average size as 11.195 nm for nanoparticles. The molecule measure of the synthesized ZNPs was in near understanding with the past discoveries[26].

4.1.2 FT-IR

The FT-IR spectra of zinc oxide is given in figure 4.2

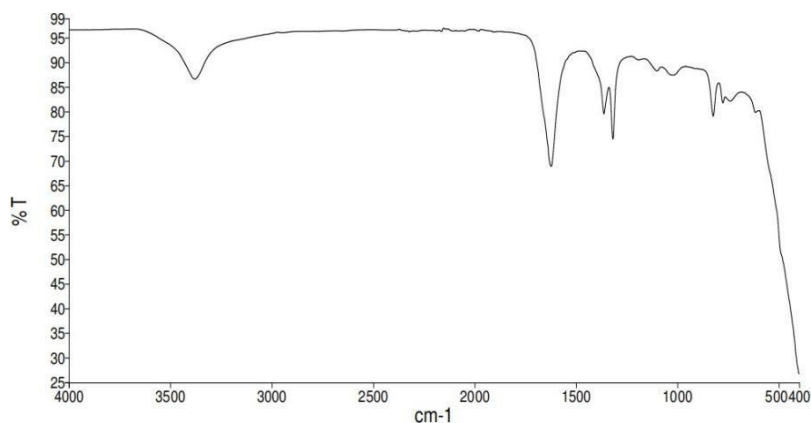


Fig. 4.2 FT-IR diagram of ZnO

In the FTIR spectra of ZnO, a sharp and intense absorption can be seen around 400 cm^{-1} . This could be due to the characteristic stretching vibration of Zn-O bond. Moreover, the peak around 1500 cm^{-1} can be ascribed due to the C-C stretching vibration and an absorption around 3400 cm^{-1} could be due to the stretching of O-H bond. These results are also in well accordance with the previous report[37].

4.1.3 HR-TEM

TEM analysis was done to understand the crystalline characteristics and size of synthesized NPs[38]. The images at different magnifications are shown in figure 4.3.

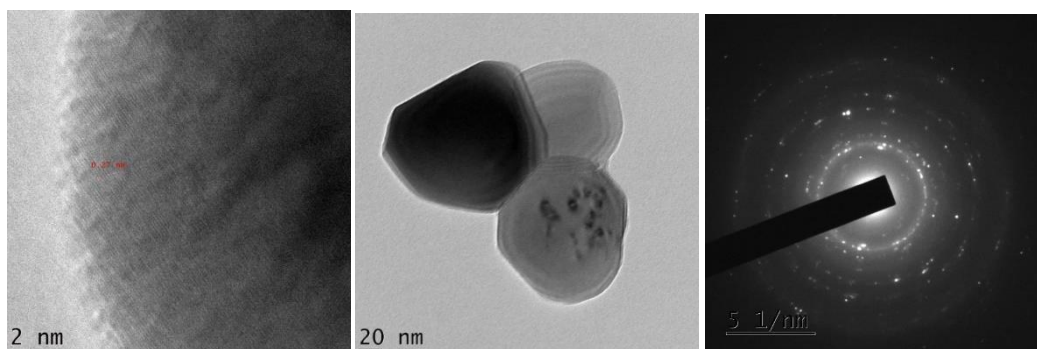


Fig. 4.3 TEM images of synthesized ZnO

4.2 CHARACTERIZATION OF GRAPHENE OXIDE (GO)

4.2.1 XRD

XRD analysis of the synthesized GO was done to determine the particle size, chemical composition, crystal structure, preferred orientation, and layer thickness of the prepared graphene oxide. The XRD pattern of the synthesized GO is shown in figure 4.4.

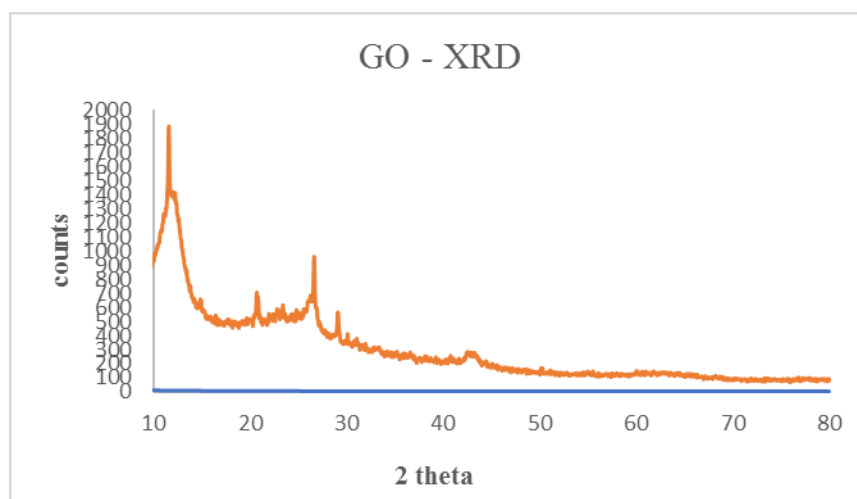


Fig. 4.4 XRD diagram of GO

It displays the graphene oxide diffraction peaks, and we obtained three peaks at $2\theta = 11.643^\circ$, 26.683° , and 29.147° , which led to the interlayer

distances of 7.59434, 3.33817, and 3.06135, proving the graphene oxide's validity[39]. Furthermore, $2\theta = 11.643$ shows that the peak is intense and pointed. We can determine the nanoparticles' crystalline size using these values. On applying the Debye-Scherrer equation to this, the crystalline size of nanoparticles can be calculated as

$$D = K\lambda / \beta \cos\theta$$

where K stands for the Scherrer constant (0.9), λ for wavelength (1.5406), β for the full width at half maximum (FWHM) of diffraction peaks in radians, and θ for the Bragg angle.

Peak 1

$$2\theta = 11.643^\circ$$

$$\theta = 5.8215^\circ = 0.1016 \text{ radian}$$

$$\beta = 0.142 = 0.0025 \text{ radian}$$

$$\lambda = 1.5406 \times 10^{-10} \text{ m}$$

From Debye Scherrer Equation,

$$D_1 = \frac{0.9 \times 1.5406 \times 10^{-10} \text{ m}}{0.0025 \times \cos(0.1016)} = \underline{\underline{55.4671 \text{ nm}}}$$

Peak 2

$$2\theta = 26.683^\circ$$

$$\theta = 13.3415^\circ = 0.2327 \text{ radian}$$

$$\beta = 0.144 = 0.0025 \text{ radian}$$

$$\lambda = 1.5406 \times 10^{-10} \text{ m}$$

From Debye Scherrer Equation,

$$D_2 = \frac{0.9 \times 1.5406 \times 10^{-10} \text{ m}}{0.0025 \times 0.9999}$$

$$= \underline{\underline{55.6471 \text{ nm}}}$$

Peak 3

$$2\theta = 29.147^\circ$$

$$\theta = 14.5735 = 0.2544 \text{ radian}$$

$$\beta = 0.162 = 0.0028 \text{ radian}$$

$$\lambda = 1.5406 \times 10^{-10} \text{ m}$$

$$\cos \theta = \cos (0.2544) = 0.9999$$

From Debye Scherrer Equation,

$$D_3 = \frac{0.9 \times 1.5406 \times 10^{-10} \text{ m}}{0.0028 \times 0.9999}$$

$$= \underline{\underline{49.5242 \text{ nm}}}$$

$$\text{Average size} = \frac{55.4671 + 55.6471 + 49.5242}{3}$$

$$= \underline{\underline{53.5461 \text{ nm}}}$$

Table 4.2 Recorded values of 2θ , d value, FWHM, particle size of XRD diffractogram

Peaks(2θ) (degree)	d value	FWHM (β)	Particle Size, D (nm)	Average Particle size (nm)
11.643	7.59434	0.142	55.4671	53.546
26.683	3.33817	0.144	55.6471	
29.147	3.06135	0.162	49.5242	

Thus, Graphene oxide has an average particle size of 53.546 nm, which guarantees that the particles are within the nanoscale. This allows us to validate that graphite can be converted into graphene oxide using a

modified Hummer's method. The peaks in the XRD pattern indicate that graphene oxide is a crystalline material.

4.2.2 FT-IR

The FT-IR spectra of graphene oxide and graphite is given in figure 4.5 and 4.6, respectively.

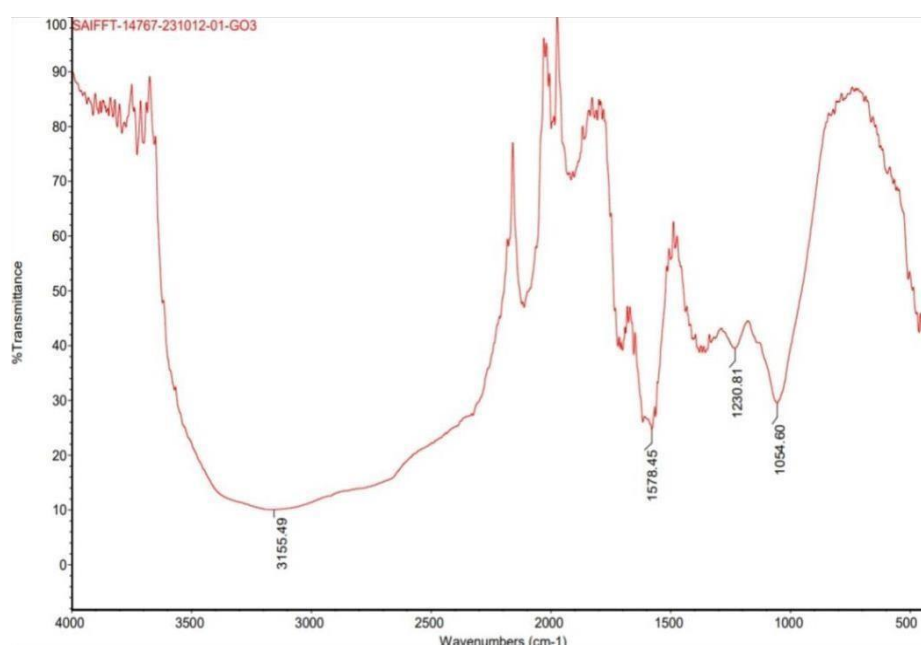


Fig.4.5 FT-IR diagram of GO

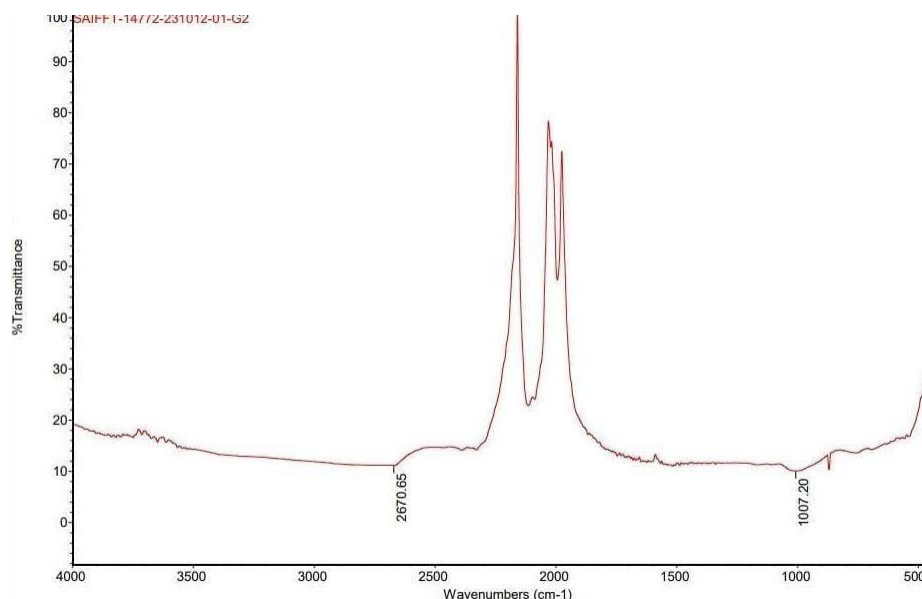


Fig. 4.6 FT-IR diagram of graphite

For graphite there are no prominent peaks but in the case of Graphene oxide, there are several peaks in the spectra showing the presence of different functional groups in graphene oxide. The FT-IR spectrum shows a broad peak between the range 3000 to 3500 cm^{-1} . The peaks at 3155.49 cm^{-1} shows the stretching vibration of O-H groups of the water molecules adsorbed on GO[39]. The sharp and intense absorption around 1700 cm^{-1} shows the presence of C=O group. Moreover, the absorption peak at 1578.45 cm^{-1} can be attributed to the stretching vibration of C=C groups. The peaks at 1230 cm^{-1} and 1054 cm^{-1} shows the presence of C-OH bonds and epoxide group (C-O), respectively.

These peaks show the presence of different oxygen containing groups on graphene oxide. Hence it can be concluded that graphite has undergone oxidation to graphene oxide.

4.2.3 HR- TEM

TEM analysis was done to understand the crystalline characteristics and size of synthesized NPs[40]. The images at different magnification are shown in Fig.4.7

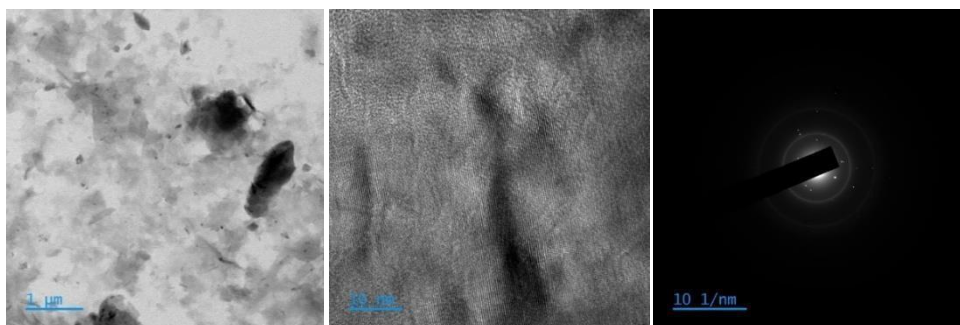


Fig.4.7 TEM images of synthesized GO

4.3 Characterization of ZnO-GO Nanocomposite

4.3.1 XRD

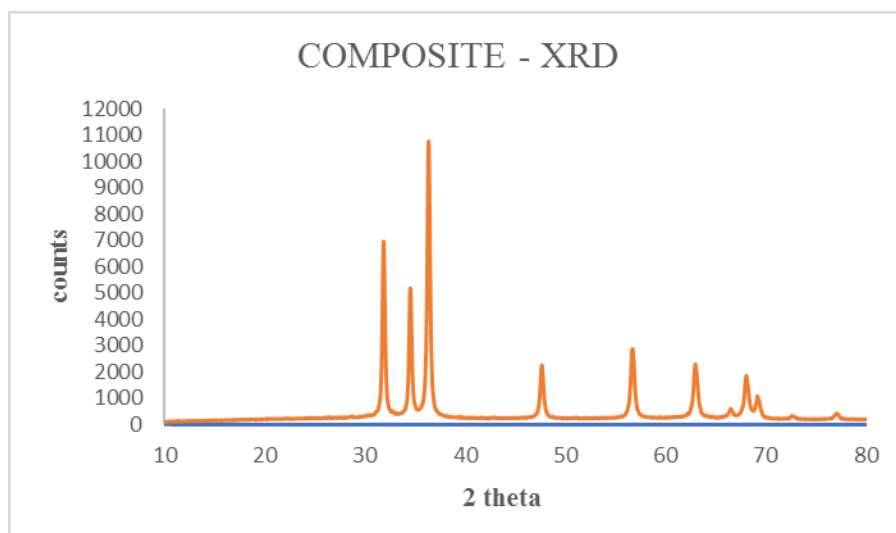


Fig 4.8 XRD diagram of ZnO-GO nanocomposite

Figure 4.8 shows the XRD patterns of the ZnO-GO nanocomposite. The crystalline formation of all samples was confirmed by fitting the obtained data using the origin software. The plains of the graph matched well with the monoclinic face of zinc oxide without any observable shift in the peak position. The intense and sharp peaks observed showed the crystalline nature of the sample. The normal crystalline measure of pure ZnO-GO was calculated by the help Debye-Scherrer's Equation: $D = k\lambda/\beta\cos\theta$, where D = crystalline size, λ = wavelength of incident X-ray , β =full width of half maximum (FWHM) of a diffraction peak, θ =diffraction angle and K = Scherrer's constant. The calculated crystalline size of the prepared composite material was around 22.722 nm. The main dominant peak with height intensity (36.337) peaks of ZnO are observed in XRD patterns of pure ZnO and ZnO-GO nanocomposites without any observable shifting.

Peak 1

$$2\theta = 31.853^\circ$$

$$\theta = 15.9265 = 0.2779 \text{ radian}$$

$$\cos \theta = 0.9999$$

$$\beta = 0.295 = 0.0051 \text{ radian}$$

$$\lambda = 1.5406 \times 10^{-10} \text{ m}$$

From Debye Scherrer Equation,

$$D_1 = \frac{0.9 \times 1.5406 \times 10^{-10} \text{ m}}{0.9999 \times 0.0051}$$

$$= \underline{\underline{27.1898 \text{ nm}}}$$

Peak 2

$$2\theta = 34.517^\circ$$

$$\theta = 17.2585 = 0.3012 \text{ radian}$$

$$\cos \theta = 0.9999$$

$$\beta = 0.302 \text{ radian}$$

$$\lambda = 1.5406 \times 10^{-10} \text{ m}$$

From Debye Scherrer Equation,

$$D_2 = \frac{0.9 \times 1.5406 \times 10^{-10} \text{ m}}{0.0053 \times 0.9999} \\ = \underline{\underline{26.16374 \text{ nm}}}$$

Peak 3

$$2\theta = 36.343^\circ$$

$$\theta = 18.1715 = 0.3012 \text{ radian}$$

$$2\theta = 47.639^\circ$$

$$\theta = 23.8195 = 0.1457 \text{ radian } \cos \theta = 0.9999$$

$$\beta = 0.323 = 0.0056 \text{ radian}$$

$$\lambda = 1.5406 \times 10^{-10} \text{ m}$$

From Debye Scherrer Equation,

$$D_3 = \frac{0.9 \times 1.5406 \times 10^{-10} \text{ m}}{0.0056 \times 0.9999} \\ = \underline{\underline{24.7621 \text{ nm}}}$$

Peak 4

$$\cos \theta = 0.9999$$

$$\beta = 0.369 = 0.0064$$

$$\lambda = 1.5406 \times 10^{-10} \text{ m}$$

From Debye Scherrer Equation,

$$D_4 = \frac{0.9 \times 1.5406 \times 10^{-10} \text{ m}}{0.0064 \times 0.9999} \\ = \underline{\underline{21.6685 \text{ nm}}}$$

Peak 5

$$2\theta = 56.689^\circ$$

$$\theta = 28.3445 = 0.4947 \text{ radian}$$

$$\cos \theta = 0.9999$$

$$\beta = 0.421 = 0.0073 \text{ radian}$$

$$\lambda = 1.5406 \times 10^{-10} \text{ m}$$

From Debye Scherrer Equation,

$$D_5 = \frac{0.9 \times 1.5406 \times 10^{-10} \text{ m}}{0.0073 \times 0.9999}$$
$$= \underline{18.9956 \text{ nm}}$$

Peak 6

$$2\theta = 62.962$$

$$\theta = 31.481 = 0.5494 \text{ radian}$$

$$\cos \theta = 0.9999$$

$$\beta = 0.452 = 0.0079 \text{ radian}$$

$$\lambda = 1.5406 \times 10^{-10} \text{ m}$$

From Debye Scherrer Equation,

$$D_6 = \frac{0.9 \times 1.5406 \times 10^{-10} \text{ m}}{0.0079 \times 0.9999}$$
$$= \underline{17.5529 \text{ nm}}$$

$$\text{Average size} = \frac{17.5529 + 18.9956 + 21.6669 + 27.1897 + 24.7621 + 26.1637}{6}$$
$$= \underline{22.7218 \text{ nm}}$$

Table 4.3 Recorded values of 2θ , d value, FWHM, particle size of XRD diffractogram

Peaks (2θ) (degree)	d value	FWHM (β)	Particle Size D (nm)	Average Particle Size (nm)
31.853	2.80715	0.295	27.1898	22.722
34.517	2.59635	0.302	26.1637	
36.343	2.47000	0.323	24.7621	
47.639	1.90738	0.369	21.6668	
56.689	1.62246	0.421	18.9956	
62.962	1.47505	0.452	17.5529	

Thus ZnO-GO Composite has an average particle size of 22.722 nm, which guarantees that the particles are within the nanoscale[39]. The peaks in the XRD pattern indicate that ZnO-GO Composite is a crystalline material.

4.3.2 FT-IR

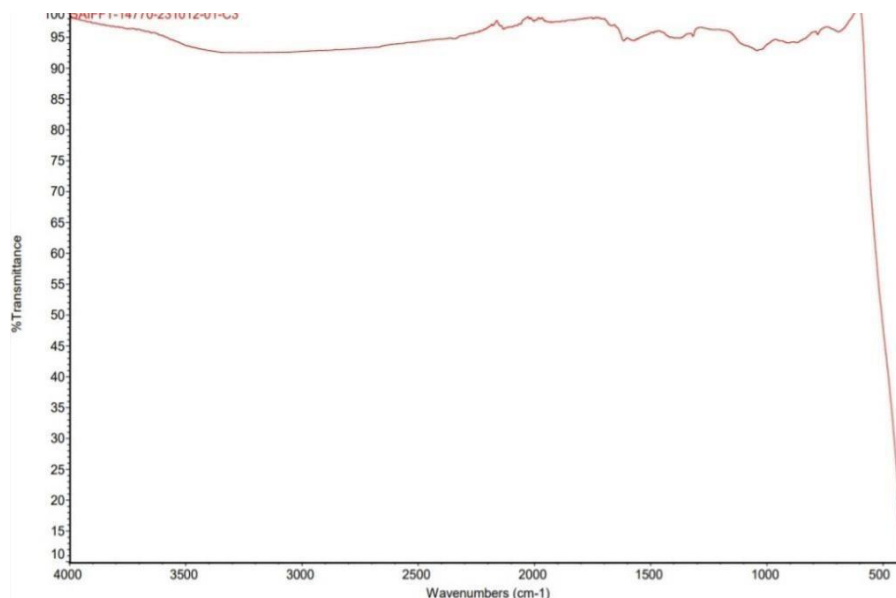


Fig. 4.9 FT-IR diagram of ZnO-GO nanocomposite

From the IR spectrum of ZnO-GO nanocomposite given as figure 4.9, it can be noted that there is a sharp and intense absorption around 400 cm^{-1} . This can be ascribed due to the stretching vibration of Zn-O bond[30]. This can confirm the presence of zinc oxide nanoparticles in the nanocomposite. Moreover, there is a marked reduction in the peak intensity of hydroxyl and epoxy groups in the spectra. All these can be attributed to the presence of ZnO on the surface of GO.

4.3.3 HR -TEM

TEM analysis was done to understand the crystalline characteristics and size of synthesized NPs[40]. The images at different magnification are shown in Fig.4.10.

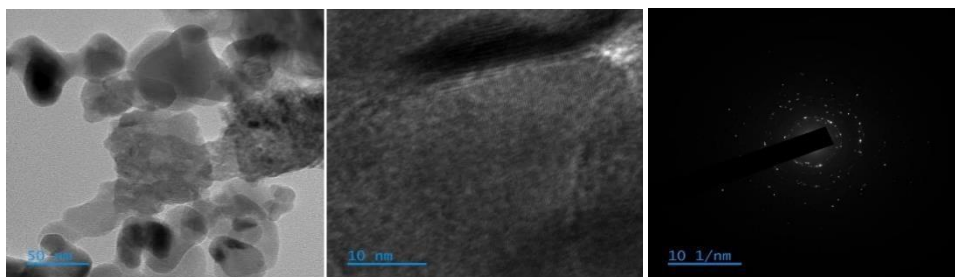


Fig 4.10 TEM images of ZnO-GO nanocomposite

4.4 PHOTO DEGRADATION OF METHYLENE BLUE

4.4.1 UV-Vis Spectroscopy

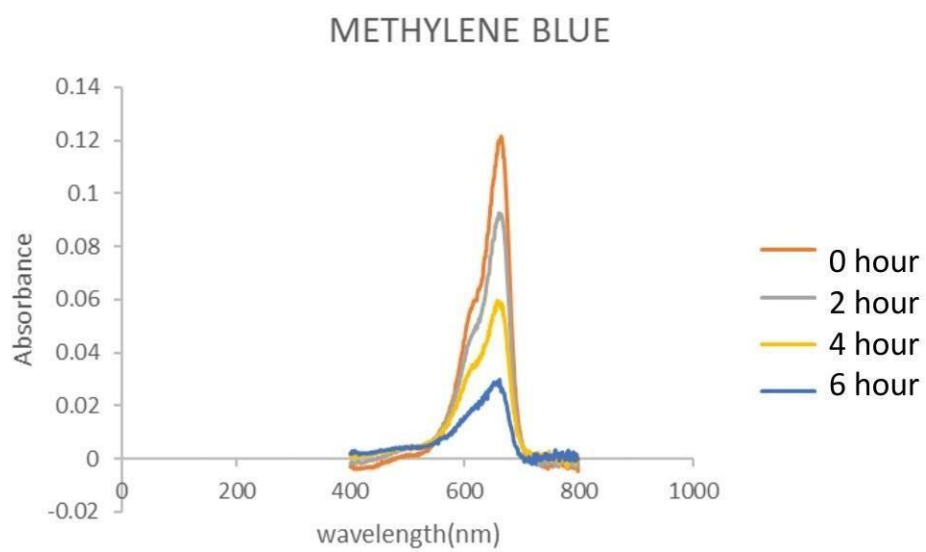


Fig 4.11 UV-Visible absorption spectrum of Methylene blue

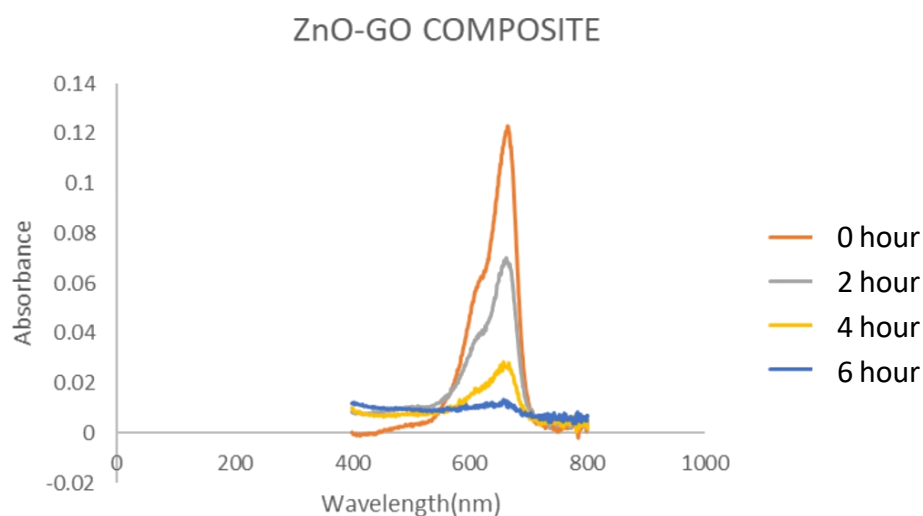


Fig 4.12 UV-Visible absorption spectrum of Zinc Oxide- Graphene Oxide composite

Figure 4.11 shows the UV-Vis spectra of MB solution before and after photo degradation. The deep blue colour of the blank MB solution remained almost same throughout the time of study. Whereas, for the mixture with the Graphene oxide, zinc oxide, composite separately, the deep blue colour of the Methylene blue solution started to fade with time. Methylene blue showed an absorption peak at 660 nm. It is clear from the graph that the absorbance of Methylene blue in the blank solution decreases only slightly with time. On the other hand, the UV-Vis spectra on the addition of Zinc oxide- Graphene oxide composite (fig 4.12) on to the Methylene blue separately showed much faster degradation. After 6 hours of exposure, it can be seen that the absorbance of ZnO- GO composite is much lower than the MB alone. This accounts for the improved photocatalytic activity of the composite due to the combined effect of Zinc oxide and Graphene oxide. Thus, it can be concluded that

the photo degradation of MB dye can be enhanced by using ZnO-GO nanocomposites[22].

4.5 ANTIBACTERIAL STUDIES

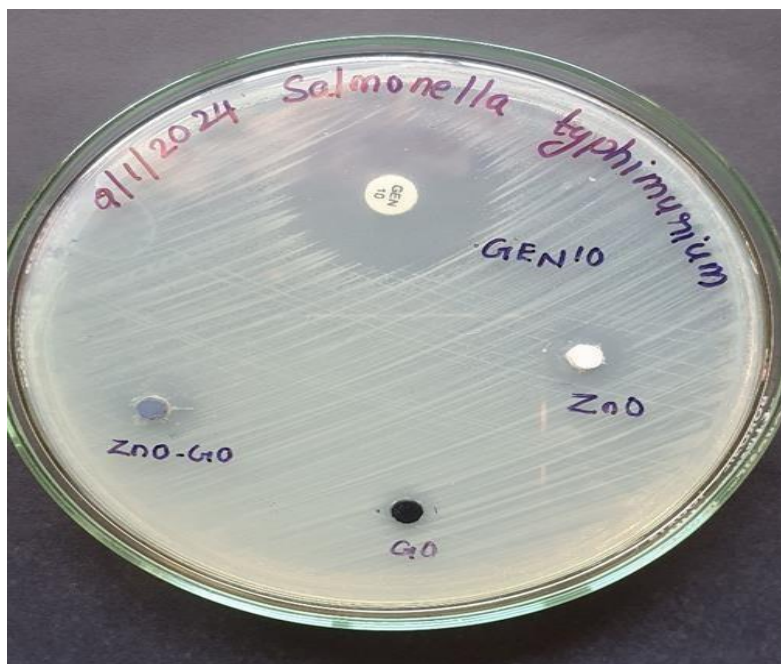


Fig 4.15 Antibacterial study done on *Salmonella Typhimurium*

Among all the results found out *Salmonella Typhimurium* (gram negative bacteria) showed accurate results in projecting out the antibacterial properties of ZnO-GO composite. *Salmonella Typhimurium* is a bacterium that causes foodborne illness in humans, known as salmonellosis. It's commonly found in contaminated food, especially poultry, eggs, and unpasteurized dairy products. Upon ingestion, the bacteria invade the intestinal epithelial cells, causing symptoms like diarrhoea, abdominal cramps, fever, and nausea. *Salmonella Typhimurium* has various virulence

Results and Discussion

factors enabling its pathogenicity, including flagella for motility and fimbriae for adhesion.



Fig 4.16 Antibacterial study done on *Bacillus Cereus*



Fig 4.17 Antibacterial study done on *Clostridium Perfringens*

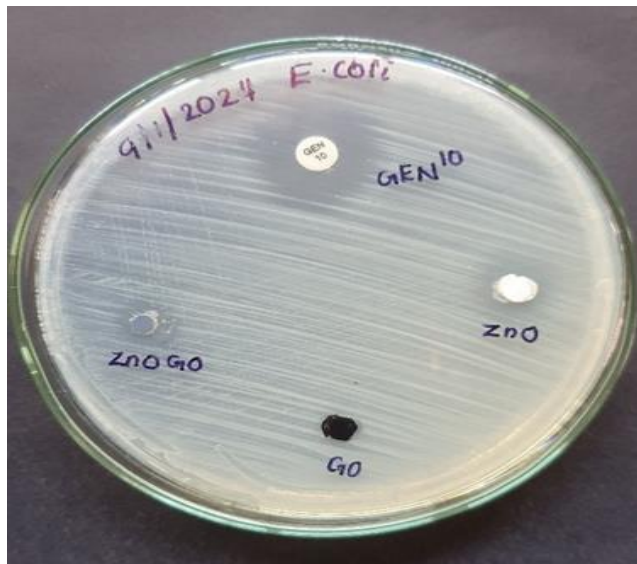


Fig 4.18 Antibacterial study done on *E. coli*

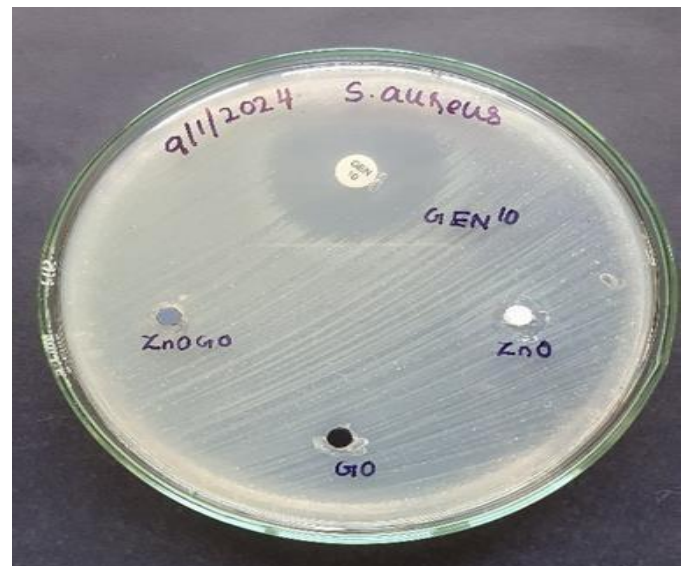


Fig 4.19 Antibacterial study done on *S. Aureus*

Table 4.4. Zone of inhibition of ZnO, GO and ZnO-GO composite

Name of the organism	Zone of inhibition in centimetres				
	Type	Sample No. 1 (ZnO)	Sample No. 2 (GO)	Sample No.3 (ZnO-GO composite)	Antibiotic disc (<i>Gentamicin</i>)
Organism 1 (<i>Clostridium Perfringens</i>)	Gram positive	1.4 cm		1.4 cm	2.4cm
Organism 2 (<i>S. Aureus</i>)	Gram positive	0.9 cm			2.5cm
Organism 3 (<i>Bacillus Cereus</i>)	Gram positive	1.3 cm			2.2cm
Organism 4 (<i>E. coli</i>)	Gram negative	1.4 cm		1 cm	2.1cm
Organism 5 (<i>Salmonella Typhimurium</i>)	Gram negative	0.9 cm	0.7 cm	1.1 cm	2.6cm

Results and Discussion

From table 4.4 it can be seen that on the incorporation of Zinc oxide nanoparticles [33] on to the Graphene oxide nanoparticles, the antibacterial properties is enhanced to a great extend in the composite compared to that the antibacterial property of Graphene oxide alone.

Chapter 5

Conclusions

In this work, the ZnO-GO nanocomposites were successfully synthesized by hydrothermal method. For this, ZnO was synthesized via green routes using *Hibiscus rosa-sinensis* leaf extract and Modified Hummer's method was adopted for the preparation of GO. From the characterizations such as XRD, FT-IR, and TEM, it can be concluded that the ZnO had been successfully synthesized and the average particle size was calculated to be around 11.195 nm. The FT-IR spectra of GO showed the presence of several oxygenated functional groups which could confirm that graphite had been oxidized to GO. From the results it can be assured that ZnO had been combined with GO to form the nanocomposites with average particle size of 22.722 nm.

The photodegradation of MB dye from water with the prepared nanocomposite was also studied under the influence of sunlight. I found out that with the ZnO-GO nanocomposites, the degradation process was much faster than that of MB alone. The antibacterial study was done by well diffusion method with bacterias like *S. Aureus*, *Bacillus cereus*, and *Clostridium perfringens* and gram-negative bacteria like *E. Coli*, *Salmonella Typhimurium*. The results showed the improved antibacterial action on GO on incorporating with ZnO nanoparticles.

The best results were showed in *Salmonella Typhimurium* with the zone of inhibition achieved from 0.7 cm for GO to 1.1 cm with ZnO-GO

composite. Thus, it can be concluded that ZnO-GO nanocomposites is a potential candidate for the photocatalytic degradation and antibacterial studies.

References

- [1] W. Zhu, P. J. M. Bartos, and A. Porro, “Application of nanotechnology in construction Summary of a state-of-the-art report,” *Mater. Struct. Constr.*, vol. 37, no. 273, pp. 649–658, 2004, doi: 10.1617/14234.
- [2] I. Khan, K. Saeed, and I. Khan, “Nanoparticles: Properties, applications and toxicities,” *Arab. J. Chem.*, vol. 12, no. 7, pp. 908–931, 2019, doi: <https://doi.org/10.1016/j.arabjc.2017.05.011>.
- [3] B. Mekuye and B. Abera, “Nanomaterials: An overview of synthesis, classification, characterization, and applications,” *Nano Sel.*, vol. 4, no. 8, pp. 486–501, Aug. 2023, doi: 10.1002/nano.202300038.
- [4] T. Joseph *et al.*, “Nanoparticles: Taking a Unique Position in Medicine,” *Nanomaterials*, vol. 13, no. 3, p. 574, Jan. 2023, doi: 10.3390/nano13030574.
- [5] V. Georgakilas, J. A. Perman, J. Tucek, and R. Zboril, “Broad Family of Carbon Nanoallotropes: Classification, Chemistry, and Applications of Fullerenes, Carbon Dots, Nanotubes, Graphene, Nanodiamonds, and Combined Superstructures,” *Chem. Rev.*, vol. 115, no. 11, pp. 4744–4822, Jun. 2015, doi: 10.1021/cr500304f.
- [6] V. B. Mbayachi, E. Ndayiragije, T. Sammani, S. Taj, E. R. Mbuta, and A. ullah khan, “Graphene synthesis, characterization and its applications: A review,” *Results Chem.*, vol. 3, p. 100163, 2021, doi: <https://doi.org/10.1016/j.rechem.2021.100163>.

References

- [7] L. Syam Sundar, M. Amin Mir, M. Waqar Ashraf, and F. Djavanroodi, "Synthesis and characterization of graphene and its composites for Lithium-Ion battery applications: A comprehensive review," *Alexandria Eng. J.*, vol. 78, pp. 224–245, 2023, doi: <https://doi.org/10.1016/j.aej.2023.07.044>.
- [8] Z. Xu and C. Gao, "Graphene fiber: a new trend in carbon fibers," *Mater. Today*, vol. 18, no. 9, pp. 480–492, 2015, doi: <https://doi.org/10.1016/j.mattod.2015.06.009>.
- [9] D. G. Papageorgiou, I. A. Kinloch, and R. J. Young, "Mechanical properties of graphene and graphene-based nanocomposites," *Prog. Mater. Sci.*, vol. 90, pp. 75–127, 2017, doi: <https://doi.org/10.1016/j.pmatsci.2017.07.004>.
- [10] M. M. Viana *et al.*, "Facile Graphene Oxide Preparation by Microwave-Assisted Acid Method," *J. Braz. Chem. Soc.*, 2015, doi: 10.5935/0103-5053.20150061.
- [11] P. H. Rana, M. Parth Modi, and M. S. Industrial, "Preparation of Graphene Oxide From Graphite Powder Using Hummer'S Modified Method," vol. 9, no. 11, pp. 305–314, 2021, [Online]. Available: www.ijcrt.org
- [12] N. A. A. Yusof, N. M. Zain, and N. Pauzi, "Synthesis of ZnO nanoparticles with chitosan as stabilizing agent and their antibacterial properties against Gram-positive and Gram-negative bacteria," *Int. J. Biol. Macromol.*, vol. 124, pp. 1132–1136, Mar. 2019, doi: 10.1016/j.ijbiomac.2018.11.228.
- [13] S. M. Mousavi *et al.*, "Recent advances in energy storage with graphene oxide for supercapacitor technology," *Sustain. Energy Fuels*, vol. 7, no. 21, pp. 5176–5197, 2023, doi: 10.1039/D3SE00867C.

References

- [14] V. Srivastava, D. Gusain, and Y. C. Sharma, "Synthesis, characterization and application of zinc oxide nanoparticles (n-ZnO)," *Ceram. Int.*, vol. 39, no. 8, pp. 9803–9808, Dec. 2013, doi: 10.1016/j.ceramint.2013.04.110.
- [15] M. N. Alam, V. Kumar, and S.-S. Park, "Advances in Rubber Compounds Using ZnO and MgO as Co-Cure Activators," *Polymers (Basel)*, vol. 14, no. 23, p. 5289, Dec. 2022, doi: 10.3390/polym14235289.
- [16] S. Sharma, D. Sharma, R. Meena, and G. A. I. O. E. Jnu-Eiacp, "A Comprehensive Overview of the Airborne Microplastics," vol. 28, pp. 16–22, Dec. 2024.
- [17] Y. Wang, J. Liu, L. Liu, and D. D. Sun, "Enhancing Stability and Photocatalytic Activity of ZnO Nanoparticles by Surface Modification of Graphene Oxide," *J. Nanosci. Nanotechnol.*, vol. 12, no. 5, pp. 3896–3902, May 2012, doi: 10.1166/jnn.2012.6174.
- [18] P. S. Kumar, P. G. N. Elavarasan, and B. S. Sreeja, "GO/ZnO nanocomposite - as transducer platform for electrochemical sensing towards environmental applications," *Chemosphere*, vol. 313, p. 137345, 2023, doi: <https://doi.org/10.1016/j.chemosphere.2022.137345>.
- [19] A. F. Ghanem, A. A. Badawy, M. E. Mohram, and M. H. Abdel Rehim, "Synergistic effect of zinc oxide nanorods on the photocatalytic performance and the biological activity of graphene nano sheets," *Heliyon*, vol. 6, no. 2, p. e03283, 2020, doi: <https://doi.org/10.1016/j.heliyon.2020.e03283>.
- [20] S. S. An, K.-S. Yun, and L. Zhong, "Graphene oxide-modified ZnO particles: synthesis, characterization, and antibacterial properties," *Int. J. Nanomedicine*, p. 79, Aug. 2015, doi: 10.2147/IJN.S88319.

References

- [21] S. Sugianto *et al.*, “Hydrothermal synthesis of GO/ZnO composites and their micromorphology and electrochemical performance,” *Int. J. Electrochem. Sci.*, vol. 18, no. 5, p. 100109, 2023, doi: <https://doi.org/10.1016/j.ijoes.2023.100109>.
- [22] R. Augustine, N. S. Kollamparambil, K. M. V, U. M., and S. Chandran A., “Silver nanoparticles: Green Synthesis using Derris trifoliata Seed Extract and It’s Applications as a Sensor, Photocatalyst and Antibacterial agent,” *Orient. J. Chem.*, vol. 39, no. 1, pp. 47–55, 2023, doi: 10.13005/ojc/390106.
- [23] B. Abebe, E. A. Zereffa, A. Tadesse, and H. C. A. Murthy, “A Review on Enhancing the Antibacterial Activity of ZnO: Mechanisms and Microscopic Investigation,” *Nanoscale Res. Lett.*, vol. 15, no. 1, p. 190, Dec. 2020, doi: 10.1186/s11671-020-03418-6.
- [24] J. K. Patra and K.-H. Baek, “Green Nanobiotechnology: Factors Affecting Synthesis and Characterization Techniques,” *J. Nanomater.*, vol. 2014, pp. 1–12, 2014, doi: 10.1155/2014/417305.
- [25] F. Sanchez and K. Sobolev, “Nanotechnology in concrete – A review,” *Constr. Build. Mater.*, vol. 24, no. 11, pp. 2060–2071, Nov. 2010, doi: 10.1016/j.conbuildmat.2010.03.014.
- [26] G. Ozcakil, “Green Synthesis of Zinc Oxide Nanoparticles by Using Pomegranate Peels: An Overview,” *Eng. Proc.*, vol. 56, no. 1, pp. 2444–2446, 2023, doi: 10.3390/ASEC2023-15280.
- [27] Y. Hou, S. Lv, L. Liu, and X. Liu, “High-quality preparation of graphene oxide via the Hummers’ method: Understanding the roles of the intercalator, oxidant, and graphite particle size,” *Ceram. Int.*, vol. 46, no. 2, pp. 2392–2402, 2020, doi: <https://doi.org/10.1016/j.ceramint.2019.09.231>.
- [28] N. Yadav and B. Lochab, “A comparative study of graphene oxide:

- Hummers, intermediate and improved method,” *FlatChem*, vol. 13, pp. 40–49, 2019, doi: <https://doi.org/10.1016/j.flatc.2019.02.001>.
- [29] N. I. Zaaba, K. L. Foo, U. Hashim, S. J. Tan, W.-W. Liu, and C. H. Voon, “Synthesis of Graphene Oxide using Modified Hummers Method: Solvent Influence,” *Procedia Eng.*, vol. 184, pp. 469–477, 2017, doi: 10.1016/j.proeng.2017.04.118.
- [30] A. R. Kachere *et al.*, “Zinc Oxide/Graphene Oxide Nanocomposites: Synthesis, Characterization and Their Optical Properties,” *ES Mater. Manuf.*, 2021, doi: 10.30919/esmm5f516.
- [31] Y. Lin, R. Hong, H. Chen, D. Zhang, and J. Xu, “Green Synthesis of ZnO-GO Composites for the Photocatalytic Degradation of Methylene Blue,” *J. Nanomater.*, vol. 2020, pp. 1–11, Aug. 2020, doi: 10.1155/2020/4147357.
- [32] H. Rehman *et al.*, “Synthesis, characterization of GO-zinc oxide nanocomposites and their use as an adsorbent for the removal of organic dyes in industrial effluents,” *Dig. J. Nanomater. Biostructures*, vol. 16, no. 4, pp. 1547–1555, 2021.
- [33] S. Gunalan, R. Sivaraj, and V. Rajendran, “Green synthesized ZnO nanoparticles against bacterial and fungal pathogens,” *Prog. Nat. Sci. Mater. Int.*, vol. 22, no. 6, pp. 693–700, Dec. 2012, doi: 10.1016/j.pnsc.2012.11.015.
- [34] M. J. Divya, C. Sowmia, K. Joona, and K. P. Dhanya, “Synthesis of zinc oxide nanoparticle from hibiscus rosa-sinensis leaf extract and investigation of its antimicrobial activity,” *Res. J. Pharm. Biol. Chem. Sci.*, vol. 4, no. 2, pp. 1137–1142, 2013.
- [35] G. Surekha, K. V. Krishnaiah, N. Ravi, and R. Padma Suvarna, “FTIR, Raman and XRD analysis of graphene oxide films prepared by modified Hummers method,” *J. Phys. Conf. Ser.*, vol. 1495, no. 1,

References

- p. 012012, Mar. 2020, doi: 10.1088/1742-6596/1495/1/012012.
- [36] W. Ma *et al.*, “Synthesis and characterization of ZnO-GO composites with their piezoelectric catalytic and antibacterial properties,” *J. Environ. Chem. Eng.*, vol. 10, no. 3, p. 107840, Jun. 2022, doi: 10.1016/j.jece.2022.107840.
- [37] S. Raut, P. V Thorat, and R. Thakre, “Green Synthesis of Zinc Oxide (ZnO) Nanoparticles Using Ocimum Tenuiflorum Leaves,” *Int. J. Sci. Res. ISSN (Online Index Copernicus Value Impact Factor)*, vol. 14, no. 5, pp. 2319–7064, 2013.
- [38] Y. T. Chung, E. Mahmoudi, A. W. Mohammad, A. Benamor, D. Johnson, and N. Hilal, “Development of polysulfone-nanohybrid membranes using ZnO-GO composite for enhanced antifouling and antibacterial control,” *Desalination*, vol. 402, pp. 123–132, 2017, doi: <https://doi.org/10.1016/j.desal.2016.09.030>.
- [39] S. Z. N. Ahmad *et al.*, “Efficient Removal of Pb(II) from Aqueous Solution using Zinc Oxide/Graphene Oxide Composite,” *IOP Conf. Ser. Mater. Sci. Eng.*, vol. 736, no. 5, p. 052002, Jan. 2020, doi: 10.1088/1757-899X/736/5/052002.
- [40] E. Salih, M. Mekawy, R. Y. A. Hassan, and I. M. El-Sherbiny, “Synthesis, characterization and electrochemical-sensor applications of zinc oxide/graphene oxide nanocomposite,” *J. Nanostructure Chem.*, vol. 6, no. 2, pp. 137–144, 2016, doi: 10.1007/s40097-016-0188-z.